Journal of ELECTRONIC MATERIALS, Vol. 46, No. 2, 2017
DOI: 10.1007/s11664-016-4988-1

Optical Properties of Rare Earth Doped SrS Phosphor: A Review

AYUSH KHARE,[1,4] SHUBHRA MISHRA,[1] D.S. KSHATRI,[2] and SANJAY TIWARI[3]

1.—Department of Physics, National Institute of Technology, Raipur 492 010, India. 2.—Department of Physics, Shri Shankaracharya Institute of Professional Management and Technology, Raipur 492 015, India. 3.—School of Studies in Electronics and Photonics, Pt. Ravishankar Shukla University, Raipur 492 010, India. 4.—e-mail: akhare.phy@nitrr.ac.in

Rare earth (RE) doped SrS phosphor has attracted a lot of attention on a wide range of photo-, cathodo-, thermo-, and electroluminescent applications. Upon doping with different RE elements (e.g., Ce, Pr, Eu, Yb), the luminescence from SrS can be varied over the entire visible region by appropriately choosing the composition of the strontium sulfide host. The main applications include flat panel displays and SrS-based powder electroluminescence (EL) for back lights. Sulfide materials known for providing Eu^{2+} based red emission band and preferred as a color conversion material in white light emitting diodes are discussed. Especially, the applications of RE doped SrS are described in light of their utility as conversion and storage phosphors. The effect of energy level splitting, EL efficiency, post-annealing, milling time, and impurity on luminescence properties for SrS are also discussed.

Key words: Optical materials, SrS:Ce, luminescence, indirect band gap, nanostructures

INTRODUCTION

Luminescence is a phenomenon that has captivated mankind for a long time. Light, emitted by glow worms, the Aurora Borealis, rotting fish, luminescent wood, and meat belongs to the family of naturally occurring luminescence. The first study of luminescent materials started in 1603. Although it is not clear which dopant or dopants are actually responsible for persistent luminescence, BaS was a largely investigated host material.[1] BaS, made accidentally, is supposed to be the first-ever synthesized sulfide phosphor. The name phosphor was already in use in ancient times, even though the chemical element phosphorous was only isolated in 1669 by the German alchemist Hennig Brand.[2] Phosphorous becomes luminescent under moist conditions upon oxidation. Thus, phosphorous is a chemiluminescent (CL) material, and the name phosphorescence, generally used for persistent photoluminescence, is inaccurate.[3] In the subsequent centuries, many scientists synthesized and investigated glowing materials, but it was too untimely for a systematic study. However, the amalgamation of CaS as a phosphor in 1700 by Friedrich Hoffmann and of SrS in 1817 by J. F. John are important to mention. Curiously enough, the luminescent properties of ZnS, which was going to become one of the largest investigated luminescent hosts in the twentieth century, were not acknowledged until 1866, when the so-called Sidot blend (hexagonal ZnS) was developed by Theodor Sidot.[4] In 1888, Eilhard Wiedemann was the first to classify different phosphors according to the type of excitation and is credited for introducing the terms luminescence, photoluminescence (PL), electroluminescence (EL), thermoluminescence (TL), chemiluminescence, triboluminescence, and crystalloluminescence.[5]

Luminescence is a spontaneous radiative recombination process involving electrons and holes.[6] The excitation of carriers prior to recombination requires an excitation source, which can be

(Received December 20, 2015; accepted September 23, 2016; published online October 24, 2016)

electrical, optical, or thermal. The luminescence triggered by an electrical excitation is known as EL, while the one taking place after the absorption of a photon is known as PL. PL is a powerful technique to probe the electronic properties of semiconductors. It involves an easy experiment and requires minimum sample preparation as, in principle, any sample capable of emitting light can be detected regardless of its thickness, geometry, or surface irregularity. It can be performed at various temperatures. Thus, it can give positive information on the temperature dependence of fundamental electronic properties, such as the energy of the band gap.[7] The PL technique can be used in conjunction with an external magnetic field to extract valuable information about the spin polarization and magneto-confinement of carriers. An applied electric field can also be used to probe the electron–hole dipole and carrier dynamics. Also, thermally activated trap levels can be studied through temperature dependent PL experiments.[8] Lasers are excellent sources of PL excitation because of their well-known unique properties such as monochromaticity and high intensity. Laser excitation energy determines the initial excited state, which is important to excite resonantly or non-resonantly the system under investigation. Laser power controls the density of excited carriers and hence the intensity of the PL spectrum. However, EL is a non-thermal light emitting process resulting from the application of an electric field to a solid substance. An uncomplicated alternating current thin-film electroluminescent (ACTFEL) device consists of metal–insulator–semiconductor–insulator–metal (MISIM) structure.

It was Destriau who first demonstrated EL in 1936. He put copper doped zinc sulfide crystals into castor oil and applied alternating current to produce light. He used power as high as 15 kW and the luminance was very poor; however, the Destriau cell triggered enormous interest in EL as the "light source of future". The early period of EL progress during the 1950s and 1960s was mainly concentrated on direct current (DC) and alternating current (AC) powder cells. It ended without much success owing to the poor performance and reliability of the devices. A few applications based on fine particles EL, for example backlight for liquid crystal display (LCDs), are proven to be attractive.[9] Many research groups were active in the research on powder EL. AC powder electroluminescent (ACPEL) devices typically consist of a doped ZnS powder suspended in a dielectric binder and sandwiched between electrodes and supported by a substrate. The substrate can be metallic or insulating. Another white reflecting coating could present additional electric protection and improve light output from the device. All LEDs have the same basic structure. For blue CL, ZnS:Ag has been the material of preference since the beginning. It has a very resourceful emission due to a donor–acceptor transition: the donor level is due to an aluminum or chlorine co-dopant and the acceptor level is due to silver.[10] This type of process shows that the emission wavelength is not determined by the nature of dopants, but by the band gap of the host. Vlasenko and Popkov,[11] simultaneously with the development of fine particle EL, presented a novel type of mechanism using a thin film phosphor. In the device they proposed, ZnS:Mn was used as an active layer which was much brighter than an equivalent fine particle EL lamp; however, the device required a very high field to operate. AC driving of the device resulted in an apparent and continuous light emission where a short light pulse was emitted corresponding to each polarity of the applied voltage. This observation led to the triel of several new activator-host combinations such as CaS:Ce (green),[12] SrS:Ce (blue-green),[13] and CaS:Eu (red)[14] and was employed successfully in $Ca_{1-x}Sr_x$S:Eu (orange to red),[15,16] $CaS_{1-x}Se_x$:Eu (orange to red),[17,18] and $SrS_{1-x}Se_x$:Ce (blue to blue-green).[19–21] In later years, attempts were made to improve the color purity, stability, and intensity of the blue part of ACTFEL phosphors. Since the largest part of sulfide phosphors were hygroscopic,[22] it was desirous to prevent the reactions with the ambient and insulating layers. Also, films prepared by physical vapor deposition (PVD) methods were sulfur deficient and amorphous due to the low sticking coefficient of sulfur and deposited at low temperature. This difficulty was overtaken by co-evaporating sulfur in presence of H_2S and post-deposition annealing treatments.

In the early 1990s, the blue emission intensity in SrS:Ce was found to be low, and hence much effort was made to find ternary sulfide hosts.[23] Ce and Eu doped $CaGa_2S_4$ and $SrGa_2S_4$ were investigated as a new class of potential thin film electroluminescent (TFEL) phosphors;[24,25] however, these materials did not provide a real breakthrough in ACTFEL technology due to the difficulty in preparing high quality thin films. Later, in 1997, SrS:Cu and SrS:Cu,Ag were investigated for the fabrication of blue-emitting ACTFEL-phosphors.[26,27] The emission from ZnS:Cu was found to result from an internal transition of the Cu ion. The progress made in this direction was unsatisfactory since the luminescence in SrS:Cu,Ag was influenced by preparational conditions of the phosphors.[21] In the coming years, several papers on the same material, consistently showing entirely different results were published. Generally, the alkaline earth sulfides (AES) in their pure form are indirect wide band-gap semiconductors, which act as luminescent materials or phosphors after doping with suitable impurities. AES phosphors find enormous applications in infrared (IR) sensors, x-ray radiation imaging plates, optical storage media, biomedical applications, radiation dosimetry, ionoluminescence, EL devices, LEDs, etc.[28] RE ion doped AES have received great attention in the phosphor display industry due to their high luminous efficiency. SrS, a member of

AES family, with a band gap of 4.2 eV, can be tuned to different emission colors by the proper choice of dopant. The PL of RE ions activated phosphors strongly depends on their valence state in the host matrix; therefore, it is essential to probe the valance state of dopants.[29]

In this review, we present an overview of the important classes of known luminescent materials based on SrS, which is a promising host material for TFEL display. Especially, SrS:Ce and SrS:Cu have been extensively studied as the blue component for multi- and full-color EL display panels.[30,31] In order to obtain blue emission from these phosphor films, a good crystallinity of the SrS host lattice is essential, since the excited levels of Ce^{3+} and Cu^{1+} centers are sensitive to the crystal field around luminescent centers.[32] Three ACTFEL phosphor host/luminescent impurity combinations, that have been elicited in most of the research and development are ZnS:Mn, SrS:Ce, and SrS:Cu. ZnS and SrS are the two most common commercial ACTFEL phosphor hosts, so it is expected that the three most studied ACTFEL systems would use these phosphors. Most of the efforts to explore these materials are geared towards developing more efficient full-color (red, green, blue) AC thin-film EL displays. Advances in TFEL technology occur rapidly due to an increasing knowledge base coupled with the interplay of developments in materials, deposition techniques, and device structures.[33] The value of threshold voltage decreases with increasing operating temperature of the EL device. It is found that the threshold voltage does not change significantly with increasing concentration of the activator in the phosphors. The aim of the present review is to provide better understanding of different optical phenomena related to SrS based blue TFEL materials, namely SrS:Eu, SrS:Ce, SrS:Cu, SrS:Cu,Ag, SrS:Eu,Sm, SrS:Pr, and SrS:Yb phosphors.

OPTICAL PROPERTIES OF IMPURITY DOPED SrS PHOSPHOR

Full Color SrS Based EL Phosphors

During the past few years, significant efforts have been made to enhance the performance of EL displays, and they are being actively researched for applications in head-mounted and automotive displays. Full-color capability is expected to be available for head-mounted applications, such as active matrix EL displays, and video graphics array (VGA) direct view panels shortly. In order to fabricate full-color TFEL devices, three primary colors (blue, green, and red) or white emitting phosphors are required; however, it is most difficult to achieve blue light emitting phosphors with appropriate color coordinates. The probable candidates for this purpose are SrS:Ce, SrS:Ce, Ag, $SrSGa_2S_4$:Ce, $CaGa_2S_4$:Ce, $BaAl_2S_4$:Eu, and ZnS:Tm, F. There are many variables affecting the development of an optimized EL phosphor. The most important is the interaction between the RE or transition metal ion activators and the host lattice, which determines the color and luminance of the device. Second is the choice of co-activators for charge compensation so as to minimize traps and non-radiative losses. The crystalline quality of the film also plays key role in maximizing EL output. The required size of columnar grains is $\sim 2\ \mu$m. This enables efficient excitation of the "hot" electrons and provides internal interfaces to minimize light piping along the film. All these properties have to be obtained in a single film and ideally grown at low temperatures so that low temperature substrates and processes can be used.[34] It was Kane et al.[35] who first reported SrS:Cu as a potential blue EL emitter. Sun et al.[36] adopted magnetron sputtering and prepared SrS:Cu EL devices and annealed them at 810°C. The luminance at 40 V showed appreciable improvement (28 cd/m^2). The resultant emission of Cu^+ centers in AES was attributed to $3d^9 4s$ (^{3}E) $\rightarrow$ $3d^{10}$ ($^1A_1$) intra-ionic transition.[37] In their study, SrS:Cu was found to be superior than SrS:Ce for fabricating full color EL displays, still almost double of EL luminous efficiency was needed for manufacturing bright VGA display. Simultaneously, to keep the production cost low, a low-temperature process was desired.

In the later investigations, $BaAl_2S_4$:Eu was found to emit blue wavelength at 467 nm. This was a result of a dipole-allowed transition from $4f^6 5d^1$ excited state to $4f^7$ ground state of Eu^{2+} ions making it the most promising blue emitting TFEL material. It were Miura et al.,[38] who first fabricated $BaAl_2S_4$:Eu thin films by dual source pulsed electron-beam evaporation. Using $BaAl_2S_4$:Eu, they demonstrated an EL intensity of the order of 65 cd/m^2 at a threshold voltage of 80 V. Color coordinates of this phosphor satisfied the requirements of blue color television displays and opened the pathway for the fabrication of full-color EL devices. In the coming years, the same group continued working on this blue emitting phosphor and reported the optical properties of blue-emitting $BaAl_2S_4$:Eu thin films for inorganic EL display.[39]

Summers et al.[34] reviewed the studies undertaken on SrS-based phosphors and extended them to develop and improve the color properties of EL displays. They achieved remarkable improvement in the crystallinity, PL and EL performance of SrS:Cu through vacuum annealing under a sulfur flow. In the two-component SrS:Cu,Ag cell, SrS:Cu was prepared by molecular beam epitaxy (MBE) and Ag^+ layer was used to compensate Ce^{3+} doping in SrS and reduce the induced Sr vacancy concentration. Figure 1 shows the variation of PL intensity with different annealing times for the samples grown under same conditions at 600°C followed by annealing at 650°C for 30 min. As is evident from Fig. 1, the PL intensity increased by a factor of almost 35. This increase was attributed to the reduction of sulfur vacancies. The best EL

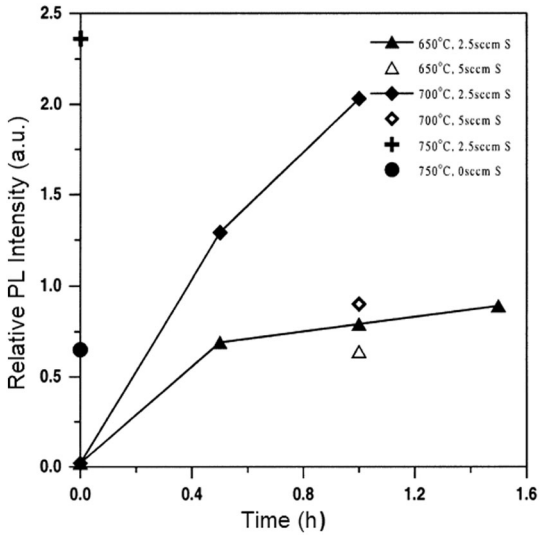

Fig. 1. PL intensity of SrS:Cu as a function of annealing time. Reprinted from "Recent progress in the development of full color SrS-based electroluminescent phosphors" by Summers et al.[34]

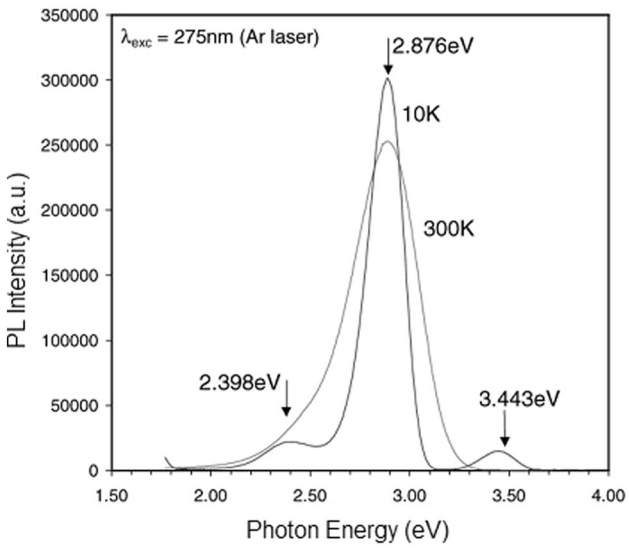

Fig. 2. PL spectra of SrS:Cu,Ag thin film at different temperatures. Reprinted from "Recent progress in the development of full color SrS-based electroluminescent phosphors" by Summers et al.[34]

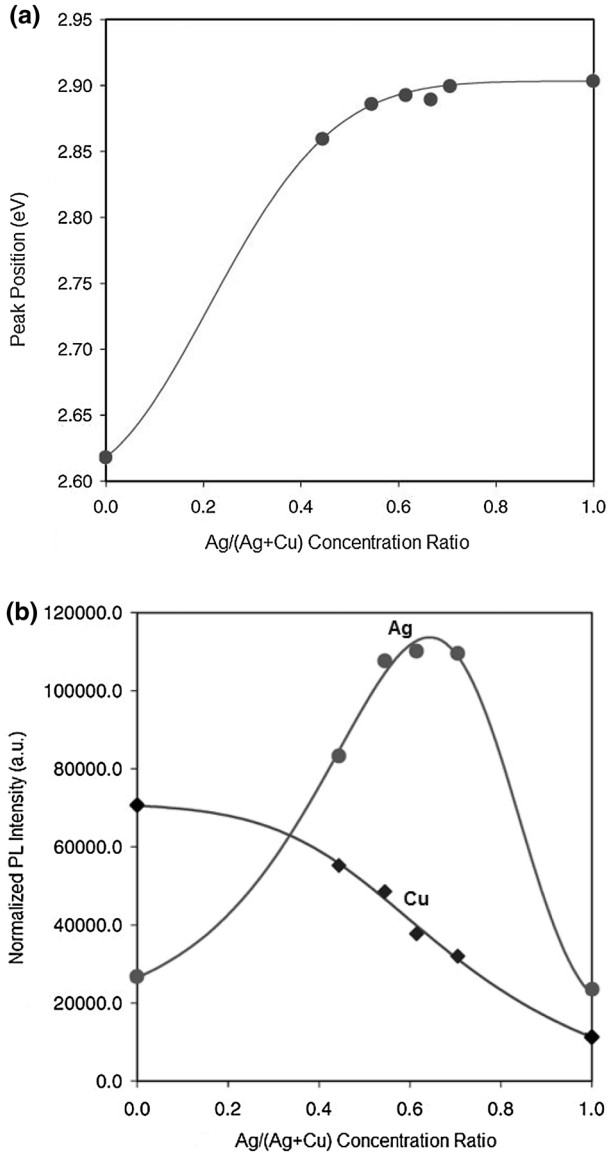

Fig. 3. (a) PL peak position of SrS as a function of Ag/(Ag + Cu) concentration ratio, (b) PL intensity of SrS:Ag and SrS:Cu phosphors as a function of Ag/(Ag + Cu) concentration ratio (λ_{Ex} = 275 nm). Reprinted from "Recent progress in the development of full color SrS-based electroluminescent phosphors" by Summers et al.[34]

performance was obtained for the sample annealed for 60 min and with international commission on illumination (CIE) coordinates of $x = 0.20$, $y = 0.32$. The PL spectra of SrS:Cu, Ag presented in Fig. 2 exhibited a deep blue color at 300 K with a peak emission at 2.876 eV (430 nm) and a line width of 390 meV that provided highly saturated blue CIE color coordinates of $x = 0.165$, $y = 0.088$. Even upon lowering the temperature to 10 K, the emission band remained unchanged and two additional emission bands were observed corresponding to 3.443 eV and 2.398 eV. When the PL spectra of singly doped SrS:Cu and SrS:Ag were compared, the two peaks obtained at 3.443 eV and 2.876 eV were attributed to emissions from Ag while the peak corresponding to 2.398 eV was analyzed to be from Cu. This observation was supported by author's earlier findings on temperature dependence of emission bands in Ag and Cu doped SrS. They found that the emission bands with Ag were independent of temperature, whereas the Cu emission band shifted towards lower wavelength at higher temperatures.[40] The authors also recorded the PL intensity of SrS phosphor at different concentration ratios of Ag to (Cu + Ag) (Fig. 3). They tried different ratios, and when it exceeded 0.44, the main emission band shifted from the Cu emission band to the Ag

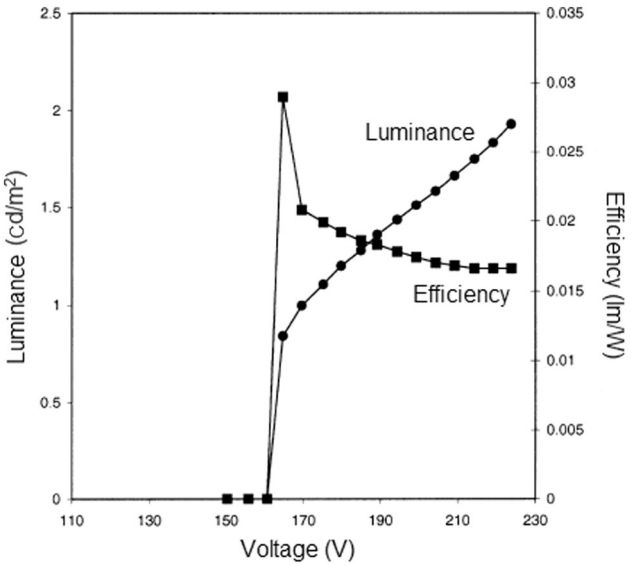

Fig. 4. SrS:Eu EL luminance and efficiency as a function of voltage. Reprinted from "Recent progress in the development of full color SrS-based electroluminescent phosphors" by Summers et al.[34]

emission band. Simultaneously, an increase in the Ag emission intensity was also noted for the ratio of 0.62; however, the Cu emission intensity monotonically decreased with increasing Ag/(Ag + Cu) concentration ratio and became half at a ratio of 0.62, as compared to singly doped SrS:Cu. This finding of enhancement of the Ag emission and the simultaneous suppression of the Cu emission in the SrS:Cu, Ag samples was indicative of energy transfer from Cu to Ag. In photoluminescence excitation (PLE) measurements Cu excitation bands appeared in the excitation spectra of the Ag emission band, directly confirmed energy transfer between the Cu and Ag ions.[34] After synthesizing the SrS systems for blue and green emission successfully, the authors extended their studies and obtained an efficient red phosphor in form of SrS:Eu. It was a red emitting phosphor with an emission band centered at 610 nm giving CIE chromaticity coordinates of $x = 0.600, y = 0.395$; however, the typical luminance and efficiency for this material were rather poor (Fig. 4).

Spectroscopic Study of SrS:Cu,Ag Thin Films

In the nineteenth century, the main objective of spectroscopic studies was to determine accurately the lines in the solar spectrum and their chemical analyses. Several spectroscopic techniques were devised, which took related research to the next level. This progress in various spectroscopic techniques also initiated rapid investigations on luminescent materials and many materials with extraordinary brilliance under cathode ray or ultra violet (UV) excitation were investigated. The excitation spectrum is recorded by varying the wavelength of the exciting light and measuring the intensity of the emitted light at a fixed emission wavelength. Just like the absorption spectrum, it also gives information on the positions of excited states. In terms of spectroscopy, the only difference is that the excitation spectrum is obtained when the emission is detected at one wavelength, and the excitation wavelength is varied while absorption spectrum is the fraction of incident radiation absorbed by the material over a range of wavelengths.[41]

One of the most exciting developments in EL phosphors in recent years is the development of SrS:Cu,Ag two-component phosphors. It was preceded and motivated by the discovery that SrS:Cu exhibited efficient EL emission with a good blue chromaticity. A detailed study of the EL characteristics of SrS:Cu,Ag phosphor showed consistency with those of SrS:Cu while the emission characteristics were identical to that of SrS:Ag.[42] After the successful synthesis of SrS:Cu, Ag by magnetron sputtering and ion assisted deposition (IAD) techniques,[43] a new class of phosphors consisting of high excitation probability and good chromaticity was reported. In this class of phosphors, the efficient coupling between the sensitizer and the activator played a critical role.

Park et al.[44] reported results of detailed spectroscopic study on the coupling mechanism between Cu and Ag ions in SrS thin films that was similar to that of their previous paper.[34] In case of SrS thin films, the emission band of Cu at 2.398 eV was observed to be suppressed due to the presence of strong energy transfer from Cu ions to Ag ions in SrS:Cu,Ag. Actually, the viability of the two-component phosphor system relies heavily on the effective coupling between the sensitizer and the activator and, therefore, it becomes imperative to understand the related mechanism.

Figure 5 shows the selective excitation PL spectra of SrS:Cu,Ag thin film at 0.4% and 0.2% concentration of Ag and Cu. The PL spectra showed three emission bands at 357.9 nm, 429.6 nm, and 515.6 nm. The first two bands at 357.9 nm and 429.6 nm were assigned to Ag ions while the band at 515.6 nm was associated to Cu emission. As can be seen from Fig. 5, the 429.6 nm Ag emission band dominated the spectrum under 278 nm excitation. Upon exciting the sample with lesser energy (310 nm), the Cu emission band at 515.6 nm became more intense and comparable with 429.6 nm Ag emission band. The 359.7 nm emission band was also found to be much weaker under 310 nm excitation. This observation was supported by slight change in decay time leading to the conclusion that suppression was due to poor direct absorption at 310 nm. Figure 6a shows the decay curves for Ag emission band at 429.6 nm. When excitation energy was reduced from 4.46 eV to 3.60 eV, the effective decay time experienced an increase from 28 s to 211 s. Thus, it was reasonable to say that the Ag emission was not seriously influenced by the change

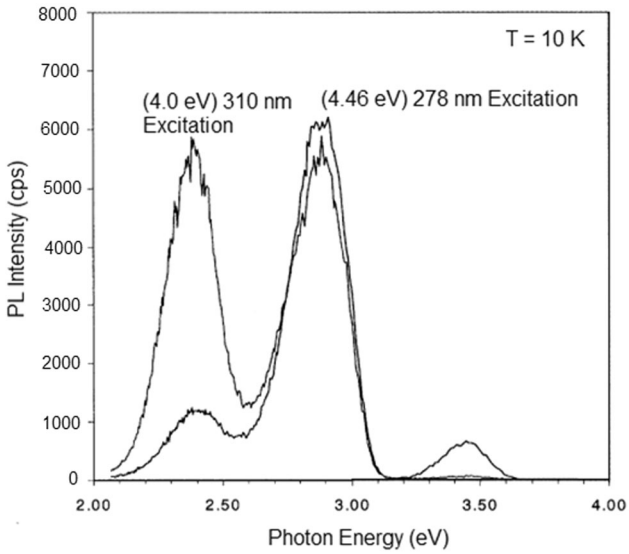

Fig. 5. Selective PL excitation spectra of SrS:Cu,Ag thin film phosphor. Reprinted from "A spectroscopic study on SrS:Cu,Ag two-component electroluminescent phosphors" by Park et al.[44]

in excitation energy. The decay of Cu luminescence at 516 nm excitation showed a drastic change upon varying the excitation energy. As shown in Fig. 6b, the effective decay time (9 μs) of the Cu emission under 277 nm excitation increased up to 80 μs when excited with lower energy (310 nm). At all excitation energies, the decay time of the Cu emission was found much smaller than that of singly-doped SrS:Cu (144 μs). This clearly indicated the presence of a mechanism that took energy away from the Cu ions and thus affected the decay rate of the Cu luminescence. This energy transfer process was most favourable for the 277 nm excitation and least favourable for the 310 nm excitation.

From above results, it was concluded that when either the activator concentration was high or when two different types of ions were present, it was possible that two ions made a simultaneous transition in which one ion was excited and the other de-excited. Such energy transfer is a commonly observed phenomenon in phosphor materials and its probability depends on the matrix element and the spectral overlap.[45]

Optical Storage and Up-Conversion Properties of SrS:Eu,Sm

Up-conversion phosphors are the materials that emit radiations of higher energies in the visible region of spectrum, when excited with IR radiation. Up-conversion luminescence is a two step process that works on the principle of electron trapping. These materials offer an inexpensive method for extending the sensitivity range to 800–1400 nm. They possess high quantum conversion efficiency and short IR response.[46] The applications of such materials to industries are many, which include

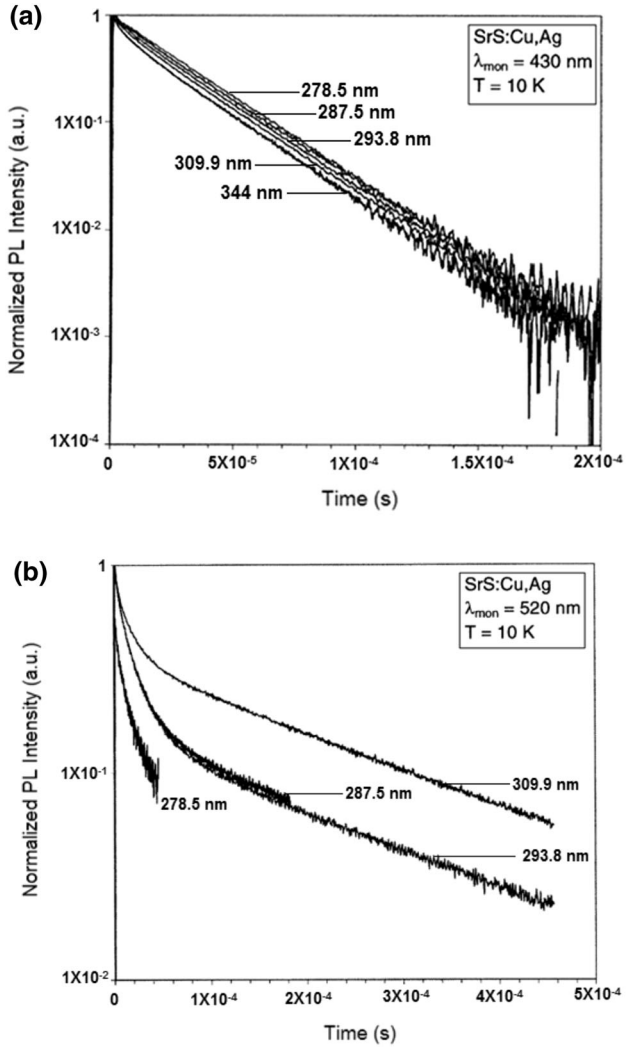

Fig. 6. Luminescence decay of SrS at various excitation wavelengths (a) Ag emission band and (b) Cu emission band. Reprinted from "A spectroscopic study on SrS:Cu,Ag two-component electroluminescent phosphors" by Park et al.[44]

detection and location of IR sources, such as vehicles, missiles, etc.[47] In last two decades, a few reports on the preparation and optical storage applications of this kind of materials were published.[46,48] Nanto et al.[49] designed a novel image storage sensor using photostimilated luminescence (PSL) in SrS:Eu,Sm phosphor. In their study, the SrS:Eu,Sm specimen exhibited an efficient PSL peak at around 600 nm upon irradiation with electromagnetic (EM) waves such as x-rays, UV, or visible rays (800–1500 nm). The PSL intensity was found to be dose dependent. This favoured the usefulness of SrS:Eu,Sm as a material for two dimensional imaging sensor for EM waves using PSL phenomenon. Later, Zhiyi et al.[50] investigated the role of Sm ions in optical storage of SrS:Eu,Sm phosphor. They found that the optical absorption lines of SrS:Eu,Sm were a result of transitions from $^6F_{5/2}$ ground state to the lower excited states ^6F and

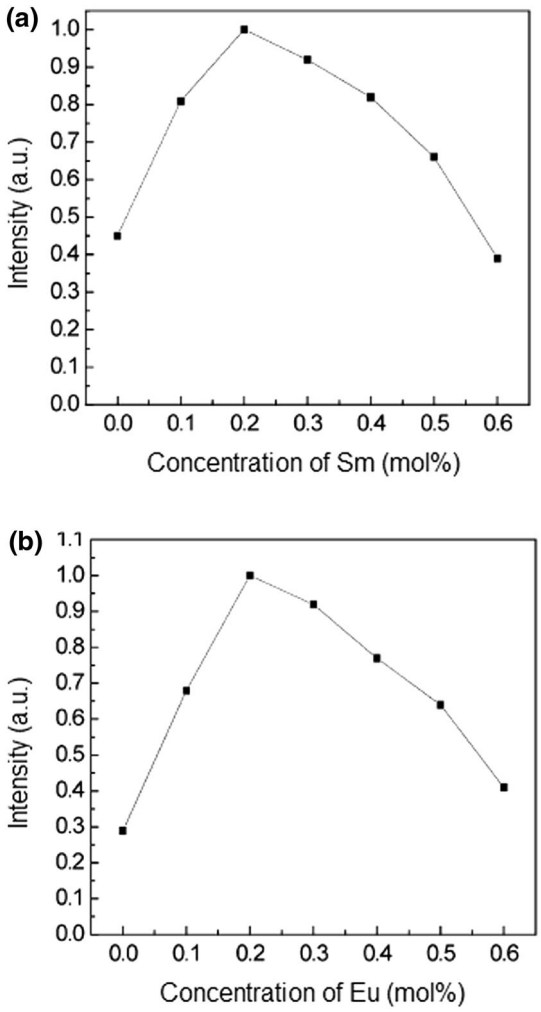

Fig. 7. Variation of up-conversion luminescence intensity with different dopant (a) Sm and (b) Eu concentration. Reprinted from "Synthesis of infrared up-conversion material SrS:Eu,Sm" by Lu et al.[51]

^{6}H within the $4f^5$ configuration of Sm^{3+}. The Sm^{3+} ions were combined with the defects such as S^- centers to form the complexes as the storing traps. They concluded also that Sm^{3+} ions did not capture electrons in the trapping process.

Lu et al.[51] synthesized Eu and Sm doped SrS up-conversion phosphors using the wet method and studied the effects of calcining temperature, calcining time, category, and concentration of the fluxing agent (LiF) and concentration of dopants on the up-conversion luminescence properties. They observed excellent up-conversion luminescence with 10% fluxing agent (LiF) and 0.2 mol% dopants (Eu and Sm). In order to optimize the concentration of activators, they prepared various samples with different concentrations of one activator keeping the other one constant. Figure 7a and b show the variation of luminescence intensity with different dopant concentrations. In the beginning the intensity increased almost linearly and became

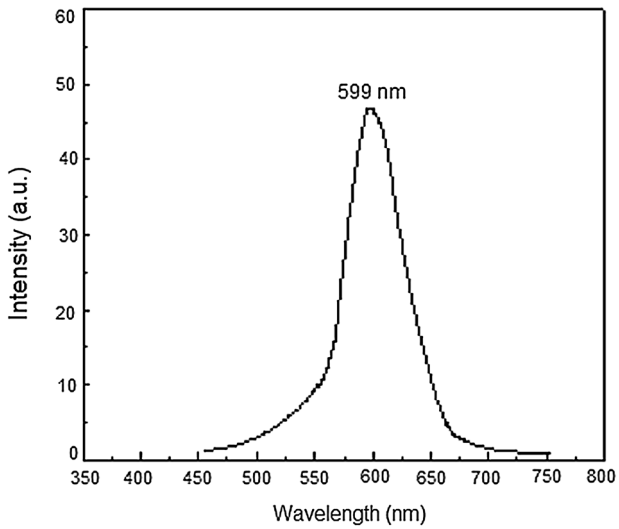

Fig. 8. Up-conversion emission spectrum of SrS:Eu (0.2 mol%),Sm (0.2 mol%). Reprinted from "Synthesis of infrared up-conversion material SrS:Eu,Sm" by Lu et al.[51]

maximum at 0.2 mol% in both cases. Thereafter, the intensity started decreasing due to concentration quenching.

Lu and co-workers calcined most intense sample SrS:Eu (0.2 mol%),Sm (0.2 mol%) at 1100°C for 1 h and exposed it to laser beam of 980 nm wavelength. Figure 8 shows the up-conversion emission spectrum of SrS:Eu (0.2 mol%),Sm (0.2 mol%) sample. As observed, it was a continuous broadband spectrum with peak at 599 nm resulted from the $5d(^2T_{2g}) \rightarrow 4f(^8S_{11/2})$ transition of Eu^{2+}. The up-conversion phosphors demonstrate TL phenomenon that also depends on the depth of traps. Generally, for the phosphors possessing up-conversion luminescence the peak temperature is higher and the trapping energy is greater. In other words, the related TL life time is longer. Figure 9 depicts the TL spectrum of the above discussed sample. No peak was witnessed throughout the temperature range indicating the presence of deeper trapping energy levels.

Luminescence Properties of SrS:Eu Single Crystal

A single crystal or mono-crystalline solid is a material in which the crystal lattice of the entire sample is continuous and unbroken to the edges of the sample with no grain boundaries. The requirements for phosphors have become more stringent, as smaller and smaller particles are required. For example, the phosphor particles used in ink jet printers have a diameter of the order of 1 μm or less so that they can be suspended in an ink formulation.[52] Smaller phosphor particles are generally desired to achieve higher resolution in computer monitors. In biology, components of a substance or objects require monodispersity along with small

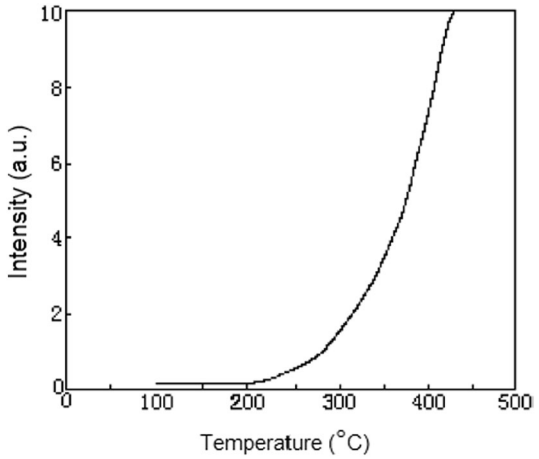

Fig. 9. TL spectrum of SrS:Eu (0.2 mol%), Sm (0.2 mol%). Reprinted from "Synthesis of infrared up-conversion material SrS:Eu,Sm" by Lu et al.[51]

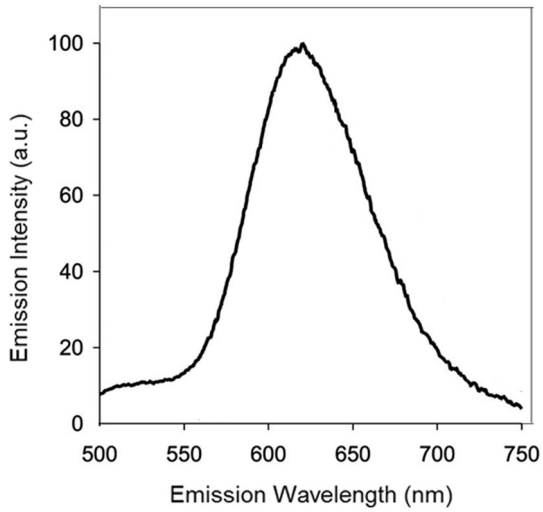

Fig. 10. PL emission spectrum of SrS:Eu crystallites. Reprinted from "Single Crystal CaS:Eu and SrS:Eu Luminescent Particles Obtained by Solvothermal Synthesis" by Van Haecke et al.[55]

particle size phosphors. The present methods for synthesis of sulfide phosphors are less efficient, and they give bulky particles of micrometer size. These conventional methods are unable to meet the challenges faced in producing nano-size particles and tailoring their properties.

Out of many existing techniques, the solvothermal synthesis method adopted by Wang et al.[53] offered several advantages. In this technique, the reaction was performed in a high-pressure autoclave. Upon increasing the solubility of the solid reactants, the reaction was speeded up and generated particles. Diffusion and growth were controlled using a suitable solvent. One of the advantages of this approach was that the reaction took place at relatively low synthesis temperature in comparison to other popular methods, such as solid-state reaction and combustion synthesis, and it was environment friendly as well. Secondly, there was not any requirement of post-deposition annealing to incorporate the Eu^{2+} ions in the AES lattice. Other methods for the preparation of SrS:Eu nanoparticles (600 nm–1.5 μm), such as co-precipitation and alkoxide methods,[54] require post-deposition treatments to obtain luminescent particles. The addition of capping agents assist in tuning the size and shape of the materials.

The suspensions prepared by Haecke et al.[55] offered good Eu incorporation and showed reasonable PL. The PL emission spectrum of SrS:Eu phosphor is presented in Fig. 10. Broad emission band peaking at 623 nm was observed for SrS:Eu. The Eu^{2+} emission was a result of transitions between the excited state (T_{2g}) of the $4f^6$ $5d$ configuration and the ground state ($^8S_{7/2}$) of the $4f^7$ configuration. Upon excitation with 450 nm wavelength, the SrS:Eu (1 mol % Eu) sample exhibited a broad PL emission band with an emission maximum at 623 nm and a full width at half maximum (FWHM) of 90 nm. The emission spectrum of SrS:Eu was comparable to that of Eu doped bulk SrS powder with an emission maximum of 620 nm and a FWHM of 76 nm at room temperature (RT).[56] Figure 11 presents the excitation spectrum of SrS:Eu crystallites for the emission at 620 nm at 70 K. The excitation spectrum consisted of three bands. The first broad excitation band (a) falling in the visible region of the spectrum was due to $4f^7 - 4f^6\ 5d^1\ (^T2_g)$ transitions of Eu^{2+} ions. The second excitation band (b) located at about 4.32 eV (286 nm) resembled the band gap energy of single crystal SrS.[57] Actually, in SrS:Eu, the Eu^{2+} environment possessed an octahedral symmetry. The crystal field splitted the $5d$ orbital into T_{2g} and E_g levels separated by the crystal field parameter $10Dq$. This was in agreement with the crystal field splitting of band at 1.49 eV suggested by Dorenbos.[58] The third band was distinguishable at about 4.8 eV (285 nm) in the excitation spectrum and was assigned to direct exciton transitions at the X point of the Brillouin zone of SrS.[59]

Defect-Assisted Green Luminescence from Doped SrS Phosphor

The luminescent properties of AES with RE ion activator have drawn considerable attention due to their potential use in cathode ray tubes (CRTs), IR sensors, TL dosimeters, EL panels, near IR to visible converters, and magneto-optical devices.[60,61] Currently, SrS phosphor is one of the most common commercial ACTFEL phosphor hosts other than ZnS:Mn. SrS:Ce,K,Eu and SrS:Pr,K are proven to be promising materials for the active layer in EL devices.[62] Although AES are one of the oldest luminescent materials; yet there is lack of information about the defect properties in these materials, especially those doped with Pr^{3+}.[63] Vacancies and defects of host materials play a vital role in

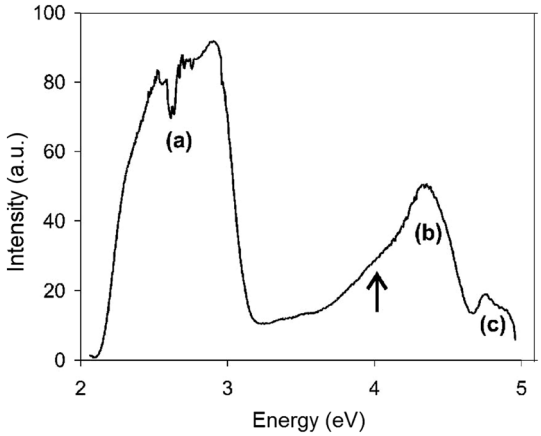

Fig. 11. Excitation spectrum of SrS:Eu crystallites. Reprinted from "Single Crystal CaS:Eu and SrS:Eu Luminescent Particles Obtained by Solvothermal Synthesis" by Van Haecke et al.[55]

luminescence centers (as electron donors and acceptors) and hold potential to exhibit wide variety of attractive luminescence features.[64] A Pr^{3+} ion is not an isovalent impurity to the metal cation Sr^{2+}. In the presence of a luminescent impurity as a donor or an acceptor and due to the large impurity concentrations ($\approx 10^{14}$–10^{20} cm^{-3}), strong perturbation of space charge neutrality occurs. This allows new electronic states to exist within the band gap, which may be associated with luminescent impurities, self-compensation induced vacancies, co-dopants, and associated defect complexes ensuring multiple applications. Materials, in their pure state exhibit band-to-band luminescence in semiconductors. If the energy levels of impurities lie in the forbidden gap, electrons, and/or holes are trapped by them and recombine with each other resulting in either radiative or non-radiative luminescence of photons.[41]

Pitale et al.[63] prepared Pr^{3+} doped SrS phosphor samples by a conventional solid state reduction method. They performed PL and thermally stimulated luminescence (TSL) studies on samples prepared at varied activator volume. They took a mixture of praseodymium oxide (Pr_6O_{11}), concentrated nitric acid (HNO_3) and distilled water in appropriate amounts (total volume 50 mL) and used different volumes of it to vary the activator concentration. The excitation and emission spectra of SrS:Pr^{3+} at different volumes (5 mL and 6 mL) of activator are shown in Fig. 12. The PL excitation spectrum of sample with 5.0 mL volume of activator consisted of a single broad band peaking at 362 nm. The corresponding emission spectrum (λ_{Ex} = 362 nm) gave a broad band at 517 nm with a shoulder around 494 nm. The PL excitation spectrum of other sample (activator volume 6.0 mL) revealed three excitation bands at 287, 314, and 355 nm while in the PL emission spectrum (λ_{Ex} = 314 nm) a band at 494 nm was observed. Since SrS was an indirect band-gap material

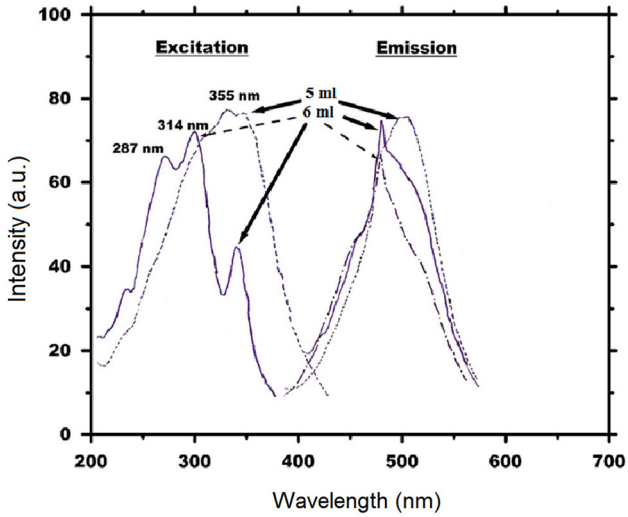

Fig. 12. PL excitation and emission spectra of SrS:Pr^{3+} at varied activator volume (5 mL and 6 mL) at RT. Reprinted from "TL and PL studies on defect-assisted green luminescence from doped strontium sulfide phosphor" by Pitale et al.[63]

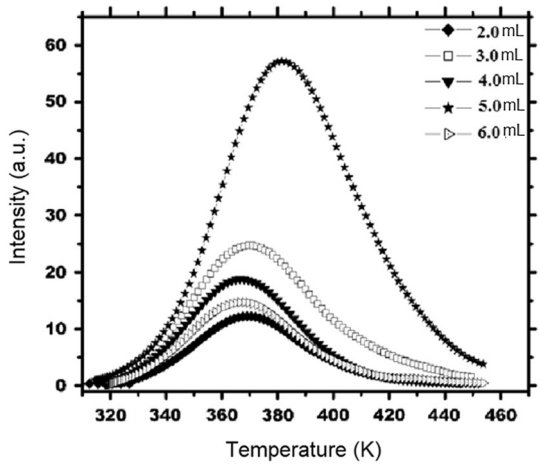

Fig. 13. TL glow curves of SrS:Pr^{3+} with varying Pr contents when irradiated with blacklight for 5 min. Reprinted from "TL and PL studies on defect-assisted green luminescence from doped strontium sulfide phosphor" by Pitale et al.[63]

(E_g = 4.20 eV), first excitation band at 287 nm was associated to the band to band transition of the host lattice and the 314–355 nm broad excitation band was attributed to transfer transition of Pr^{3+}-S^{2-}. The PL spectra of samples with other volumes (2.0–4.0 mL) of activator were found similar to the spectrum obtained for sample with 5.0 mL of activator volume except for a few variations in the emission intensities.

Figure 13 presents the TL glow curves of UV irradiated SrS:Pr^{3+} sample at varied activator volume (2.0–6.0 mL). As it was seen, all curves showed a broad single peak in the temperature range from 365 K to 382 K. In all the cases, TL intensity rose with temperature, became maximum at a particular

temperature, and then decreased at still higher temperatures. It was further noted that for 2.0 mL and 3.0 mL activator volume, the TL peak intensity increased. At 4.0 mL activator concentration, it decreased and became maximum for 5.0 mL activator volume. Finally, TL intensity was quenched with further increase in activator concentration (6.0 mL). The decrease in intensity was supposed to be due to greater number of non-radiative transitions. Out of five samples, the TL intensity was observed to be maximum for sample with 5.0 mL of activator volume at 382 K. According to previous reports on the AES phosphors, the TL peaks observed by various workers for SrS hosts doped with different activators mostly fell in the temperature range of 325 K to 375 K where the trapping states were primarily assigned to natural defects of the host.[65]

Advances in Sulfide Phosphors for Displays and Lighting Applications

Recent developments in display technology have initiated tremendous efforts in optimizing suitable luminescent materials. This has led to a large number of phosphors, which are perfect for display applications. Cost reduction and controlling levels of unwanted impurities are other issues to be addressed. An essential condition to get highly efficient phosphors is to prepare chemicals with highest possible purity before doping necessary amount of activator into it.

Sulfide-type phosphors are produced from pure ZnS or CdS or their mixtures by heating them together with small amounts (0.001–0.1%) of copper, silver, gallium, or other salts, which are generally called activators, and with about 2% of sodium or another alkali chloride at about 1000°C. The role of the alkali halides is to facilitate the melting process and to serve as co-activators or fluxes. Even a very small amount of it plays a decisive role as far as luminescence efficiency is concerned. Copper-activated ZnS and CdS exhibit a rather long afterglow when their irradiation ceases, which is favourable for applications in radar screens and self-luminous phosphors. The peaks in the emission spectrum of zinc sulfide are reported to shift towards longer wavelength side when substitution of zinc ions by cadmium ions increases.[66]

Poelman et al.[67] elaborately reported about $Ca_{1-x}Sr_xS$:Eu single crystal particle phosphor. They developed the material by solvothermal synthesis, which did not require toxic gases or high temperature processing steps. The goal of the their work was to develop single crystalline Eu-doped $Ca_{1-x}Sr_xS$ particles. This phosphor is generally preferred in LEDs because it combines a broad excitation and red-emission spectrum.[67] The solvothermal growth procedure was employed for synthesis (crystallite size 1–2 μm) of both CaS:Eu and SrS:Eu phosphors.[55,68] From the emission spectrum (Fig. 14), it was found that the Eu-ions (mainly in a 2^+ valency state) were

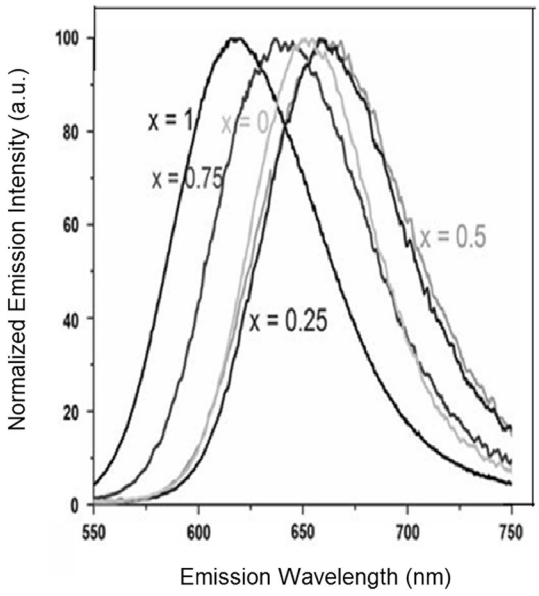

Fig. 14. PL emission spectra of $Ca_{1-x}Sr_xS$:Eu as a function of particle composition. Reprinted from "Advances in sulfide phosphors for displays and lighting" by Poelman et al.[67]

actually incorporated into the particles and not on their surface. The thioglycerol used as a capping agent in this case not only assisted in capping the particles, but also controlled their size and separation. In its presence as a catalyst, the particle growth was highly uniform and gave almost monodisperse single crystalline particles representing an octahedral form with (111) face of the sulfide lattice. As is known, Eu doped CaS is an efficient deep red phosphor in which the PL spectrum peaks at 655 nm. This luminescent emission was associated to $5d$–$4f$ transition of Eu^{2+} (Fig. 14). Since this emission was slightly extended towards near IR red region, the eye sensitivity for this type of light was reasonably low; however, by slightly decreasing the crystal field on the Eu^{2+} sites, the luminous efficacy of radiation (LER) was found to increase when emission spectrum shifted to lower wavelength side peaking at 620 nm. It is important to state that the spectrum was not saturated enough, and hence was not appropriate for many applications. Therefore, a spectrum intermediate between CaS:Eu and SrS:Eu was suggested to be an ideal choice. Since, CaS and SrS possessed same crystallographic structure, they were mixed and synthesized for bulk powders[69] and thin films.[70] Figure 15 shows the PL emission spectrum upon excitation at 450 nm. In order to obtain optimum emission spectrum for red emission, $Ca_{0.25}Sr_{0.75}S$:Eu composition was tried that peaked at 640 nm. It is imperative to mention here that this phosphor possessed an apparent brightness to the human eye, which was about 53 percent higher than that of CaS:Eu. Although, the band gap excitation was quite inefficient, the broad excitation band from about 400-550 nm corresponding to direct excitation

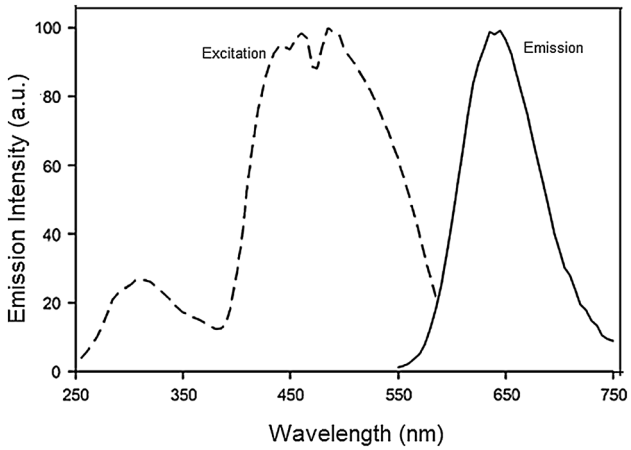

Fig. 15. PL excitation (dashed) and emission (full line) spectra of $Ca_{0.25}Sr_{0.75}S$:Eu. Reprinted from "Advances in sulfide phosphors for displays and lighting" by Poelman et al.[67]

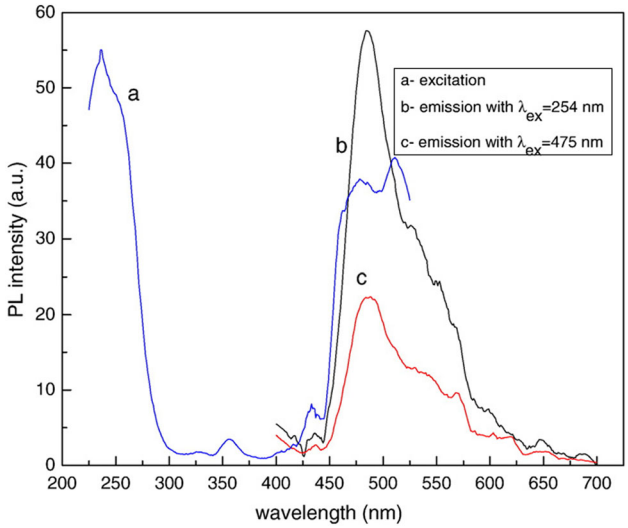

Fig. 16. PL excitation and emission spectra of SrS:Ce^{3+} nanocrystalline phosphor. Reprinted from "Synthesis of Ce^{3+} doped SrS nanocrystalline phosphors using a simple aqueous method" by Kumar et al.[72]

of the Eu^{2+} ions was very intense and made this type of phosphor material ideally suitable for wavelength conversion of blue LEDs.[67]

PL of SrS:Ce Nanocrystalline Phosphor

Nanoscience is the study of manipulation of materials at molecular, atomic, and macromolecular scales, where properties are significantly different from those at a superior scale. Nanotechnology is the characterization, production, designing, and application of structures, systems, and devices by calculating the shape and size at nanometer scale. These techniques comprise of a wide range of tools, techniques and applications. The size of interest typically ranges from atomic level to 100 nm. As is known, materials in this range, especially at the lower end, exhibit enhancement in different properties in comparison to corresponding bulk phase. These materials bridge the gap between amorphous materials without any long range order and crystalline materials with a clear three dimensional long range order. Nanoparticles are larger than individual atoms and molecules but are smaller than bulk solids. There are two main phenomenona responsible for variation in various properties: (1) the high dispersity of nanocrystalline systems and (2) size quantization. Dispersity is a measure of the heterogeneity of sizes of molecules or particles in a mixture. As the size of a crystal is resolute, the number of atoms at the plane of the crystal increases in comparison to the number of atoms in the crystal. In the nano phase, the properties determined by the molecular structure of the bulk lattice gradually become more dominating by the defect structure of the surface. The second phenomenon, called as size quantization is the property of metals and semiconductors that produces changes in the microscopic properties of the material due to quantization of confined carrier motion. As a result of spatial confinement of the charge carriers, the valance and conduction bands are splitted into discrete and quantized electronic levels, which are parallel to those in atoms and molecules. Because of the above discussed, two distinctive phenomena occurring in nanoparticles, their electrical, optical, chemical, mechanical, and magnetic properties, can selectively be tailored by altering the size, morphology, and composition of the particles.[71]

A similar work was carried out by Kumar et al.,[72] who applied a simple aqueous method to synthesize a blue–green emitting Ce^{3+} doped SrS nanocrystalline phosphor where $SrCl_2$, $Na_2S_2O_3$ and $Ce(NO_3)_3$ were used as precursors for Sr^{2+}, S^{2-} and Ce^{3+} ions respectively. The utility of aqueous method lies in the fact that it is a low cost, less time consuming, more productive, non-toxic and environment friendly. The calculated average particle size was 27 ± 2 nm. Figure 16 shows the excitation and emission spectra of the SrS:Ce^{3+} nanocrystalline phosphor. An intense peak at 480 nm accompanied by a shoulder at 527 nm was witnessed as a result of the transition from the 5*d* state to the 4*f* $^2F_{7/2}$ state of the Ce^{3+} ion. Two excitation peaks at 254 nm and 475 nm were also obtained for emission of the SrS:Ce nanocrystalline phosphor. In the bulk SrS:Ce phosphor, generally the emission occurs at 485 nm and 530 nm.[73] Thus, a shift towards the lower wavelength side, compared to bulk SrS:Ce phosphor was observed by Kumar et al. Here, it is important to mention that SrS possessed a rock-salt structure, where Ce^{3+} ion replaced the Sr^{2+} ion exhibiting a sixfold coordination. Since the 4*f* state of the Ce^{3+} ion was shielded from the influence of the surroundings, the crystal field caused a small perturbation of the 4*f* state, which was negligible in comparison to spin–orbit interaction. It is well

established that the energy level of the $^2T_{2g}$ state of the excited 5*d* electrons of the Ce^{+3} is sensitive to its surrounding crystal field.[74] The Ce^{3+} has a $^2F_{5/2}$ ground state, which separates the next excited state $^2F_{7/2}$ by 2200 cm^{-1}. The interesting result the authors witnessed was that upon excitation with 254 nm, the SrS:Ce nanocrystalline phosphor showed an emission peak at 480 nm having intensity three times of the peak obtained at 475 nm excitation. The authors claimed that this feature of SrS:Ce might be valuable in using it as a scintillator for the gamma or x-rays, in high-energy physics as a track detector and also in medical field.[75] The targeted applications were the measurement of the dose delivered during a treatment in radiation therapy and the monitoring of the dose or dose-rate around or in nuclear reactor and accelerator facilities in high energy physics.

White-Light LEDs: Exploration of AES Phosphors

The breathtaking development of white LEDs in recent years has led to significant market potential for a range of brand new applications. The high efficiency of these LEDs means solutions for room lighting and backlighting for LCD displays can be realized now. The advantages of their reduced energy requirements are apparent. For example, the running time of battery operated devices such as mobile phones and notebook computers can be extended considerably. Many research groups are engaged in exploring this fast growing field of white LEDs. Among others, work by Suresh et al.[76] highlighted the study of red and orange emissions of CaS:Eu^{2+} and SrS:Eu^{2+}. They investigated the effects of doping concentration on luminescent properties of CaS:Eu^{2+} and SrS:Eu^{2+} by exciting the samples with EL blue LED (460 nm) and employing them as coating layer for fabricating white LEDs. The broadband excitation and emission spectra of these phosphors were seen as the typical emission of Eu^{2+} ions attributed to the 4*f* to 5*d* transitions. These phosphors were found capable to fulfill the requirements for blue LED chips due to their broadband absorption in the visible region (400–630 nm). This group successfully fabricated a white-light LED through the integration of a 460 nm chip validating the employment of these phosphors as potential candidates for the application in blue LED chip-based white-light LEDs.

Figure 17 displays the excitation spectrum of SrS:Eu^{2+} at different wt% monitored under 650 nm wavelength. The broadband excitation peaks of 5*d* field splitting components e_g and t_{2g} shifted towards longer wavelength side in the region from 250 nm to 285 nm and a blue shift to a region from 390 nm to 585 nm as shown in Fig. 17. The red shift was observed due to ligand and field splitting of 5*d* level of Eu^{2+} for both emission and excitation peaks from CaS host to SrS host. A single

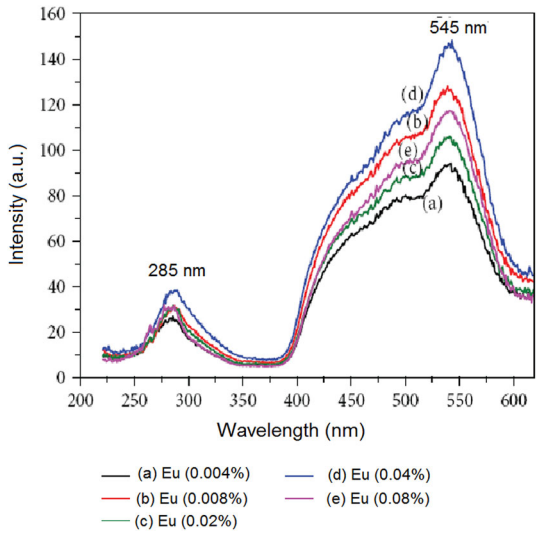

Fig. 17. Excitation spectra of SrS:Eu^{2+} at different wt%, monitored under 650 nm wavelength. Reprinted from "Rare earth doped alkali earth sulfide phosphors for white-light LEDs" by Suresh et al.[76]

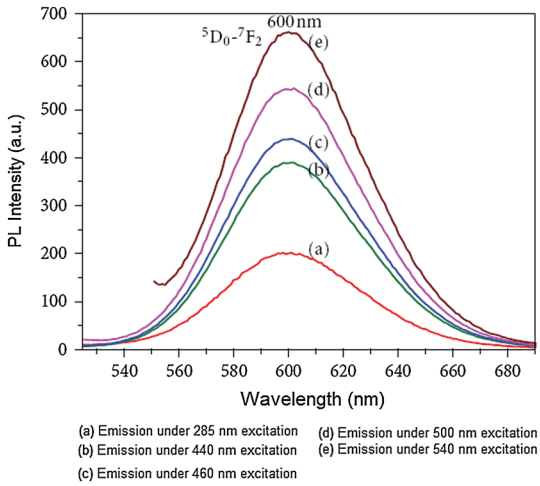

Fig. 18. Emission spectra of SrS:Eu^{2+} phosphor (0.04 wt%) under different excitation wavelengths. Reprinted from "Rare earth doped alkali earth sulfide phosphors for white-light LEDs" by Suresh et al.[76]

broadband emission of Eu^{2+} in SrS was observed shifting towards shorter wavelength (600 nm) as shown in Fig. 18. Since SrS has a halite (cubic) structure that makes it easier to have a solid solution in order to adjust the positions of absorption and emission bands and obtain better color rendering for white LED applications.[77]

PL of Pulsed Laser Deposited (PLD) SrS:Ce Quartz Thin Film Nanophosphor

There are many advantages of thin film phosphors over the conventional powder phosphors. They include high resolution, uniformity, thermal stability, and lower susceptibility to charging.[78]

Several researchers reported on the synthesis of SrS based thin films on different substrates using, for example, PLD,[79] electron beam evaporation,[80] radio frequency (RF) sputtering,[81] atomic layer epitaxy, etc.[82] Since electrons and holes are spatially confined in low dimensional systems causing quantum confinement effects, energy levels, and hence optical properties are considerably different from their bulk counterparts.[83] This observation has generated a considerable interest in exploring nanomaterials both in powder[84] and thin film forms.[85] Powder form of SrS based nanophosphors has been investigated in detail recently.[86]

In their recent work, Vij et al.[87,88] used laser deposition technique and reported the effect of nanostructure formation on the band gap of thin film nano-phosphor using UV spectroscopy in absorption mode. In their studies the average grain size estimated from atomic force microscopy (AFM) measurement was found to be nearly 40 nm. The details of UV-absorption spectroscopy have already been discussed in "Spectroscopic Study of SrS:Cu,Ag Thin Films" section of this article. The absorption coefficient (α) and the band gap (E_g) are related as follows[89]

$$\alpha h\nu = \left(h\nu - E_g\right)^n, \tag{1}$$

where α is the optical absorption coefficient near the fundamental absorption edge, $h\nu$ is the photon energy, and n has a value of 1/2 for direct band gap and 2 for an indirect band gap materials. Figure 19a shows the absorption spectrum and Tauc's plot for nanocrystalline SrS:Ce thin film. Tauc's plot was obtained by extrapolating the linear portion of the graph between incident photon energy and $(\alpha h\nu)^{1/2}$. The point where the straight line crosses the X-axis gives the band gap value. The band gap value was calculated to be 4.52 eV, which was blue shifted in comparison to the band gap (4.20 eV) of its bulk counterpart.[90] The shift in band gap towards blue region signified the formation of nanostructure[91] and was attributed to the quantum size effect (QSE).[92] Other factors responsible for such shifting could be film thickness, grain size or even the presence of different phases. QSE is one of the most direct effects that appears upon reducing the material size to the nanometer range.

Figure 19b shows the PL spectra of the nanocrystalline SrS:Ce thin films grown at 400°C and 500°C. The spectra comprised a broad band peaking at 466 nm along with a shoulder at around 515 nm. The authors assigned these emission bands at 466 and 515 nm to the well-known 5*d*–4*f* transitions of Ce^{3+} levels.[90] The similar interpretation was given by Kumar et al.[72] for shielding of 4*f* state of the Ce^{3+} ion from the influence of the surroundings. It is essential to mention that in comparison to microcrystalline thin film, the PL emission in the case of nanocrystalline thin film was significantly blue shifted.[93] One more thing that deserves attention

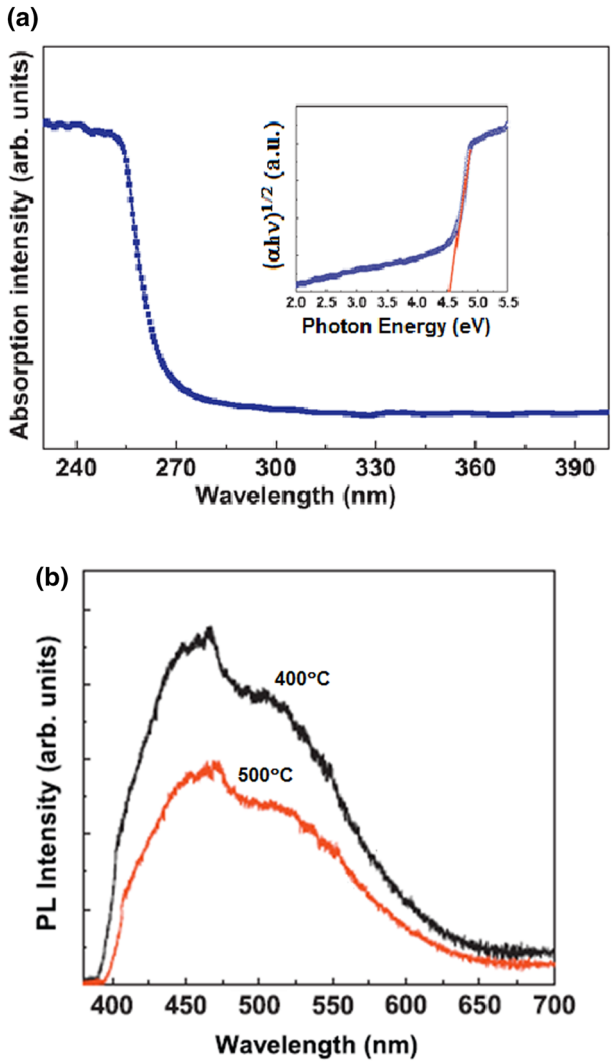

Fig. 19. (a) Absorption spectrum of single phase SrS:Ce thin film. Inset shows the corresponding Tauc's plot. (b) The PL spectrum of SrS:Ce thin film grown at different temperatures. Reprinted from "Blue shift in band gap and photoluminescence of pulsed laser deposited SrS:Ce/quartz thin film nanophosphors" by Vij et al.[88]

is that apart from a slight blue shift in emission wavelength, the PL output of the film grown at 400°C was almost 1.6 times higher than the film grown at 500°C. Authors compared the PL spectrum of thin film nanophosphor with SrS:Ce powder phosphor also.[90] Though, the blue shift in PL was seen for SrS:Ce thin film nanophosphor; however, the PL was almost six times lower than that obtained in powder phosphor. A similar type of observation was reported by Huttl et al.,[94] who obtained that PL yield for SrS:Ce,Cl thin film was around five times lower than that for powder. In semiconductor materials, the luminescence mechanism is generally explained in terms of recombination of electrons in the conduction band and holes in the valence band. As the band gap widens, these materials show a blue shift in the luminescence spectrum due to quantum confinement.[87] The blue

shift in PL was explained on the basis of phenomenological crystal-field model,[95] which stated that the luminescence shift for Ce doped matrix depended on two parameters: the shift of energy centroid (E_c) in the 5*d* orbit and the effect of crystal field splitting.[87] As the crystalline size approached nano order, the bond distance between Ce^{3+} ions and the host matrix also decreased raising the centroid and t_{2g} energy levels. As a result, the changes of energy levels in the centroid and t_{2g} shifted the emission spectrum towards shorter wavelength. Since SrS was a wide band gap semiconductor material and was unable to show luminescence in visible region, the presence of Ce in SrS was confirmed by PL spectroscopy.

Effects of Ce^{3+} Doping on the Optical Properties of SrS Nanoparticles

Recently, we have reported our various findings concerning the effects of Ce^{3+} doping on the structural and optical properties of SrS nanoparticles.[96–98] We synthesized Ce^{3+} doped SrS phosphor using solid state diffusion method (SSDM).[99] This is a method in which the particle size depends on the uniformity of grinding and homogeneity of the sample. The band gap values were determined by recording the absorption spectra of different nanocrystalline SrS:Ce^{3+} (0.1%, 0.25%, 0.5%, 0.75%, and 1%) powder samples in the wavelength range from 200 nm to 500 nm at RT (Fig. 20a). The absorption bands corresponding to different SrS:Ce^{3+} samples were located between 260 nm and 270 nm. The reported[89] experimental band gap value (E_g) for SrS:Ce^{3+} is 4.54 eV; however, the band gap values for different nanocrystalline SrS:Ce^{3+} (0.1%, 0.25%, 0.5%, 0.75%, and 1%) phosphor samples as extracted from Tauc's plots (Fig. 20b) were found to be 4.72 eV, 4.74 eV, 4.75 eV, 4.77 eV, and 4.78 eV. As the dopant concentration was increased, it created additional donor levels at the bottom of conduction band and the Fermi level slightly shifted towards conduction band. In such a situation of wider energy gap, the electrons requied more energy to move from valence band to conduction band and thus the effective optical band gap was greater. Based upon the above results, it was concluded that SrS:Ce was an indirect band gap material.

The excitation spectra (Fig. 21a) was spread in the wavelength range from 250 nm to 550 nm. Two main peaks were observed at 375 nm and 320 nm. The first peak at 320 nm was due to the band-to-band absorption in the host lattice while the main peak centered at 375 nm was attributed to the direct absorption in the dopant ion levels within the band gap. This suggested the possibility of excitation of SrS:Ce by UV light and Sunlight. As a clear observation, the highest doped (0.5%) SrS:Ce^{3+} sample showed maximum excitation intensity

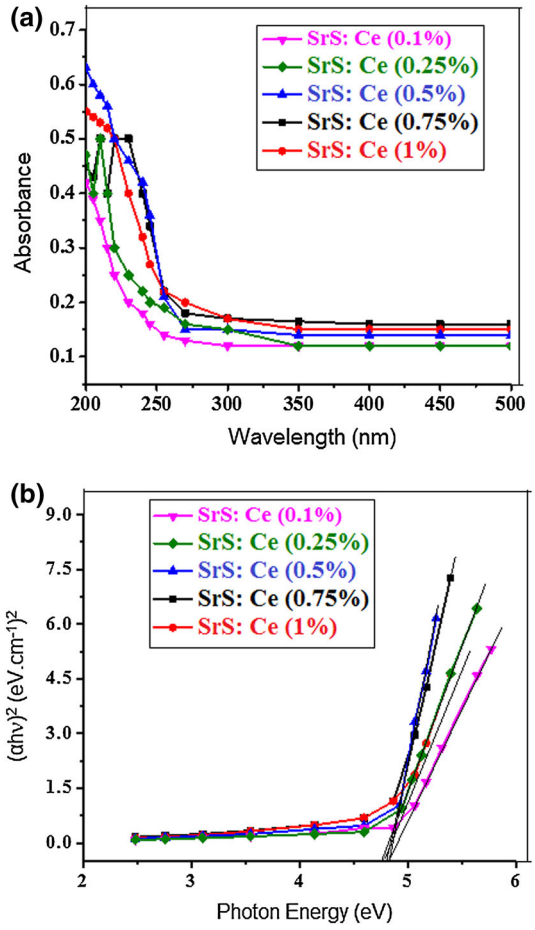

Fig. 20. (a) Absorption spectra and (b) Tauc's plots of different $Sr_{(1-x)}S:Ce^{3+}_x$ (x = 0.001, 0.0025, 0.005, 0.0075, and 0.01) nanophosphors. Reprinted from "The effects of Ce^{3+} doping on the structural and optical properties of SrS nanoparticles synthesized by solid state diffusion method" by Mishra et al.[96]

supporting the suitability of 0.5 mol% of Ce^{3+} ions to create luminescence center.

In the emission spectra (Fig. 21b), once again two intense peaks were seen. The first peak observed at 459 nm was accompanied by emission of blue light while the second shoulder peak recorded at 551 nm was accompanied by green light. These peaks were a result of transition from the excited $^2T_{2g}$ of 5*d* state to $^2F_{5/2}$, $^2F_{7/2}$ of 4*f* ground state of the Ce^{3+} ion.[100] The alike results were reported by Thiyagarajan et al.[101] who obtained similar PL emission spectra for SrS:Ce prepared by the solid state carbothermal reduction technique at 900°C for 5 h. The above mechanism could be understood on the basis of energy level diagram presented in Fig. 22.

We have investigated the effect of high energy ball milling (HEBM) on different optical properties of SrS:Ce^{3+} phosphors also. The excitation (λ_{em} = 459 nm) and emission (λ_{ex} = 375 nm) spectra of unmilled and milled (3 h, 6 h, and 10 h) SrS:Ce^{3+} (0.5 mol%) nanophosphor are depicted in Fig. 23a and b, respectively. Upon exposing the phosphor

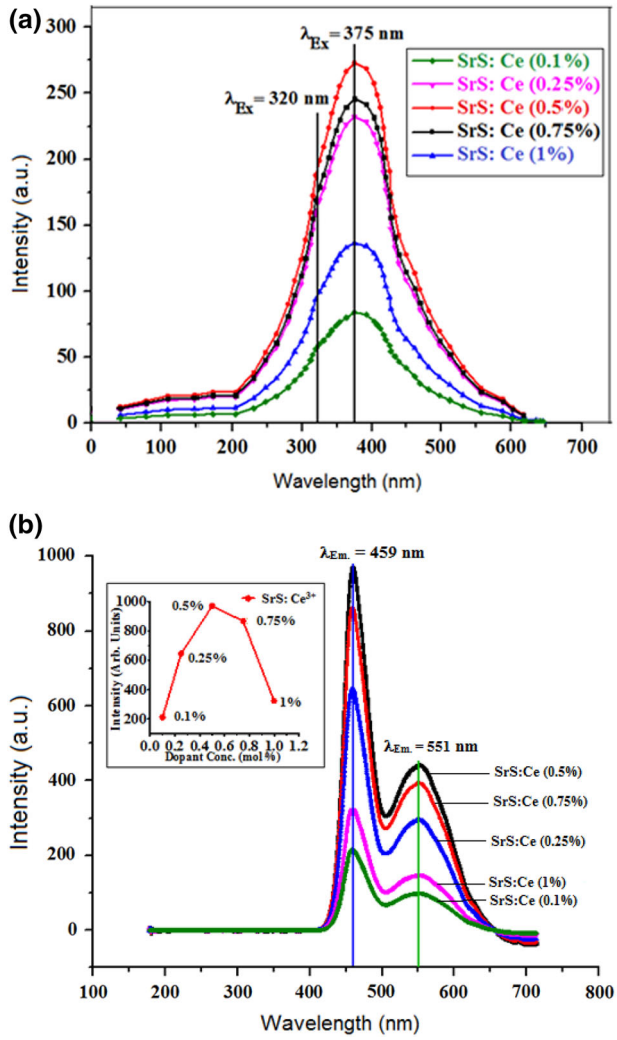

Fig. 21. (a) PL excitation (λ_{Em} = 459 nm) and (b) emission (λ_{Ex} = 375 nm) spectra of different SrS:Ce^{3+} (0.1%, 0.25%, 0.5%, 0.75%, 1%) nanophosphors. Reprinted from "The effects of Ce^{3+} doping on the structural and optical properties of SrS nanoparticles synthesized by solid state diffusion method" by Mishra et al.[96]

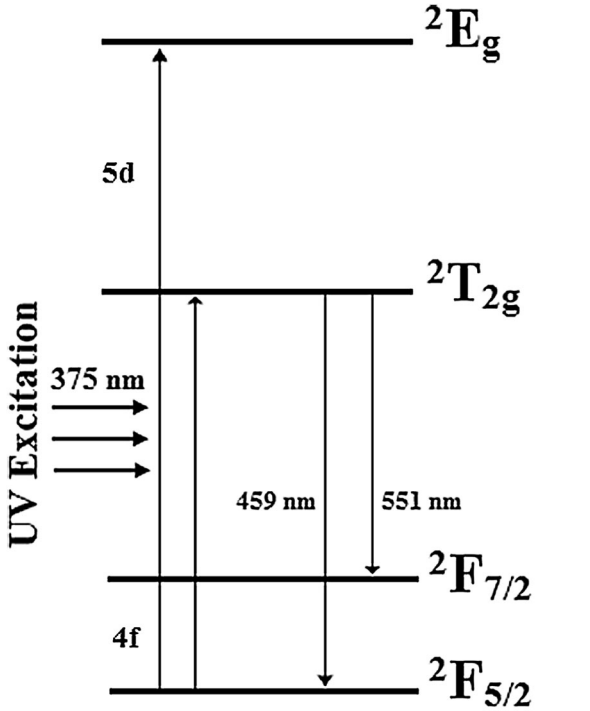

Fig. 22. Energy levels of a Ce^{3+} ion in crystal field for 4*f* and 5*d* configurations at RT. Reprinted from "The effects of Ce^{3+} doping on the structural and optical properties of SrS nanoparticles synthesized by solid state diffusion method" by Mishra et al.[96]

samples to UV light (375 nm), SrS host lattice absorbed incident photons as a result of which electron–hole pairs were created and charge migration took place through trapping and recombination resulting in PL. It was observed that Ce^{3+} as dopant was responsible for creating different kinds of emission centers in host matrix.[102] The excitation spectra of unmilled and milled samples exhibited a strong absorption in the band range from 200 nm to 550 nm peaking twice; a very weak band at 320 nm and a highly intense band at 375 nm attributed to $4f \rightarrow 5d$ transitions of Ce^{3+} ions.[97] The exclusive feature of excitation spectrum of SrS: Ce^{3+} phosphor was the strong absorption in blue region, which made it a potential applicant for LED fabrication and related studies.[103] When the sample was milled for 3 h, the relative PL intensity decreased. For other milled samples (6 h and 10 h), the PL intensity decreased further and became minimum for 10 h milling. In other words, as the particle size decreases the relative PL intensity decreases.[104] This decrement in PL intensity was associated to QSE that arose due to nanocrystalline nature of studied samples. Another feature of QSE, the blue shift in peak positions was not very appreciable in the present case.[105] The same behavior was witnessed by Yuan et al.[106] where emission intensity of $NaYF_4$:Yb,Er particles decreased with increasing milling time. Recently, Hernandez et al.[107] studied the effect of high energy dry milling on luminescence of strontium aluminates and observed similar response. They correlated the decrease in PL intensity with significant damage in crystallites and surface particles.

Figure 23b shows the PL emission spectra of different unmilled and milled (3 h, 6 h, and 10 h) nanophosphor samples exhibiting a broad emission band in the wavelength range from 350 nm to 650 nm at a predetermined excitation wavelength of 375 nm. The emission spectrum of unmilled SrS:Ce^{3+} phosphor consisted of the most intense peak at 459 nm (blue region) with a shoulder peak at around 551 nm (green region) due to the direct excitation of the dopant levels within the band-gap. These emission bands were again attributed to the transitions of Ce^{3+} ions from the lowest 5*d* ($^2T_{2g}$) excited energy level to the 4*f* ($^2F_{5/2}$,$^2F_{7/2}$) ground energy levels within the host SrS matrix.[96] This was in accordance with Russell–Saunders coupling approximation.[100] The related transition

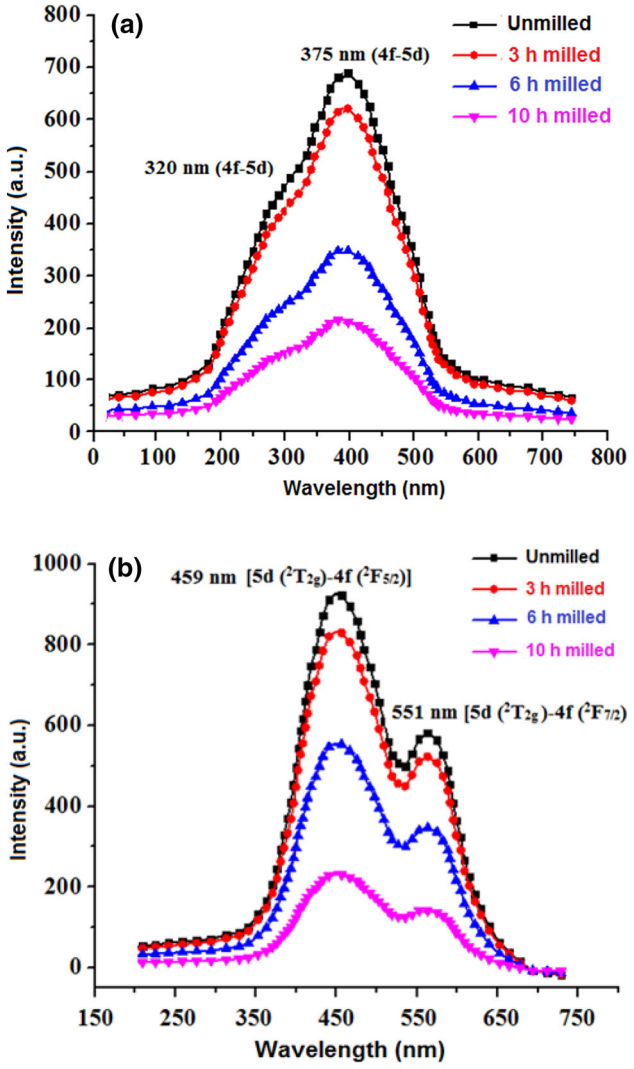

Fig. 23. (a) PL excitation (λ_{Em} = 459 nm) and (b) PL emission (λ_{Ex} = 375 nm) spectra of unmilled and milled SrS: Ce^{3+} (0.5%) sample.

mechanism of Ce^{3+} ions already discussed in "PL of SrS:Ce Nanocrystalline Phosphor" section is shown in Fig. 22.[108,109] The PL emission intensity also followed the same pattern. It was maximum for unmilled sample and decreased with increasing milling time.

Persistent Luminescence from SrS:Yb^{+2} Phosphor

Recently, there has been great concern over storage phosphors.[110] These materials are capable of absorbing and storing energy under the excitation with sunlight or artificial light sources and releasing it for appreciable time even after the excitation source is withdrawn.[111–113] Their applications mainly involve in emergency lighting and safe traffic, various displays and signing applications.[114,115] The mechanism on which these phosphors behave as energy storage materials is the

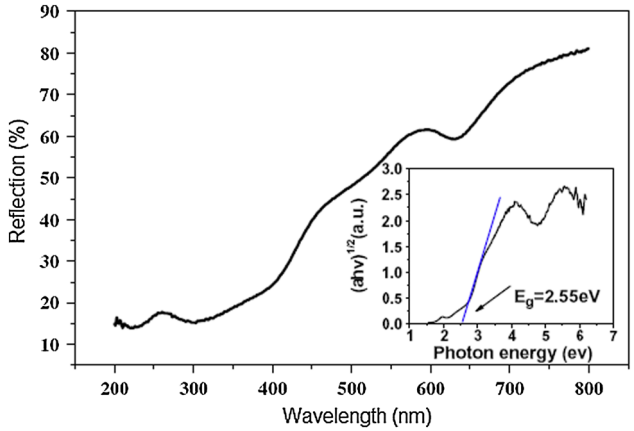

Fig. 24. Diffuse reflection spectra of SrS:Yb^{2+} (0.5%). The inset shows the optical energy-gap (E_g) of SrS:Yb^{2+} (5%). Reprinted from "A novel Yb^{2+} doped SrS long persistent luminescence phosphors" by Yang et al.[110]

generation of carriers (electron and hole) trap centers.[116] If the traps are shallower, long persistent luminescence (LPL) is witnessed at RT while for deeper traps PSL is observed.[117] SrS doped with RE elements such as Eu^{2+}, Sm^{3+}, Ce^{2+} has been explored as storage phosphor in the recent past. Apart from traditional RE dopants, some other lesser known RE elements have also been used by many researchers. One such RE dopant is ytterbium (Yb), the penultimate element in the lanthanide series with +2 oxidation state. Yang et al.[110] reported a new red emitting phosphor SrS:Yb^{2+} synthesized by solid state reaction technique (SSRT). They recorded diffuse reflection spectrum and estimated the band gap of SrS:Yb as 2.55 eV using Tauc's plot method (Fig. 24). Their estimation was found to match with the results (band gap = 2.54 eV) obtained from generalized gradiant approximation (GGA).[118] It is well established that GGA usually gives band gap values slightly lower than the experimental ones.[119] The reason was the incapability of GGA in reproducing both exchange–correlation energy and its charge derivative accurately. Engel and Vosko[120] tried to rectify this deficiency and suggested a new functional form of the GGA, which reproduced the exchange potential at the expense of less agreement in exchange energy. This approach called as EVGGA explained band splitting and some other properties, which depended mainly on the accuracy of exchange–correlation potential in a better way.

In the PL studies (λ_{Ex} = 273 nm), the emission spectra of SrS:Yb consisted of four bands around 378, 470, 540 and 605 nm (Fig. 25). When first three peaks were monitored, the excitation spectra were found to exhibit only one band ranging from 250 nm to 300 nm and peaking at 273 nm; however, while monitoring at 605 nm, the excitation spectrum contained two bands around 273 nm and 465 nm as shown in Fig. 25. Thus, it was inferred that the

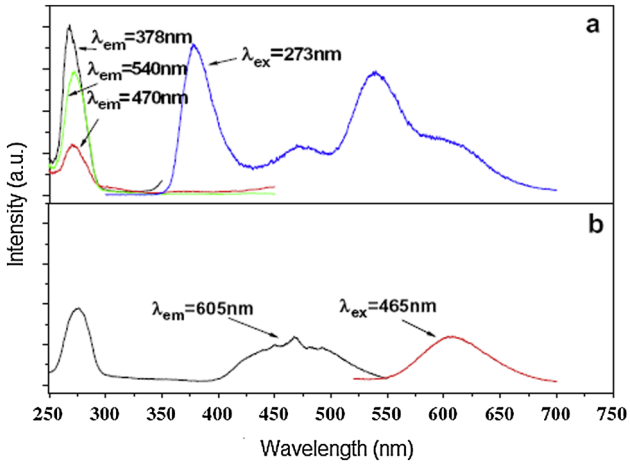

Fig. 25. (a) The PL spectrum of SrS:Yb^{2+} (5%) at excitation wavelength of 273 nm and the excitation spectra monitored at 378, 470, and 570 nm, respectively. (b) The excitation spectra at 605 nm and the PL spectrum at excitation wavelength monitored at 465 nm. Reprinted from "A novel Yb^{2+} doped SrS long persistent luminescence phosphors" by Yang et al.[110]

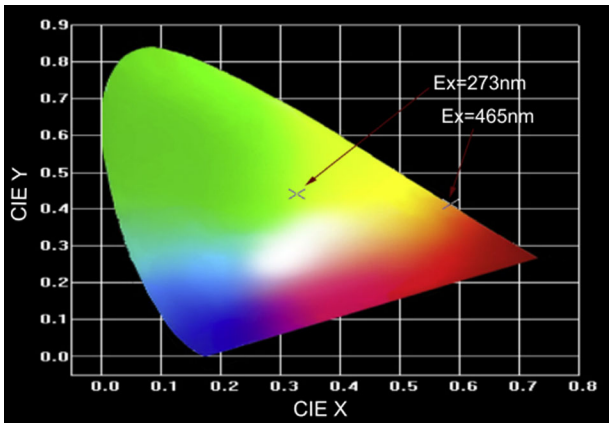

Fig. 26. The CIE chromaticity diagram of SrS:Yb^{2+}. Reprinted from "A novel Yb^{2+} doped SrS long persistent luminescence phosphors" by Yang et al.[110]

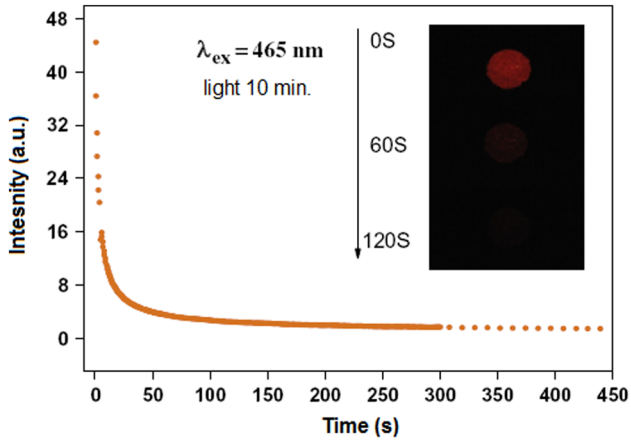

Fig. 27. The afterglow decay curves of SrS:Yb^{2+} phosphor excited at 465 nm. Reprinted from "A novel Yb^{2+} doped SrS long persistent luminescence phosphors" by Yang et al.[110]

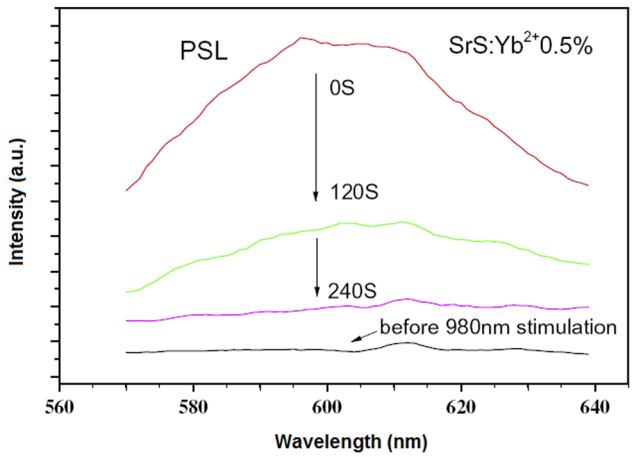

Fig. 28. The PSL emission spectra of SrS:Yb^{2+} at different stimulation times after the removal of the radiation source (10 min). Reprinted from "A novel Yb^{2+} doped SrS long persistent luminescence phosphors" by Yang et al.[110]

emission peak situated at 470 nm transmitted a part of energy to the emission at 605 nm. The authors estimated CIE coordinates using the spectral energy distribution of the SrS:Yb^{2+} phosphor. The CIE chromaticity diagram for PL of SrS:Yb^{2+} at excitation wavelengths of 273 and 465 nm is presented in Fig. 26. The calculated values were $x = 0.321$, $y = 0.543$ and $x = 0.586$, $y = 0.412$, respectively.

One of the encouraging findings of Yang et al.[110] was that SrS:Yb^{2+} showed red LPL upon excitation with 465 nm light. As shown in Fig. 27, the luminescence intensity decayed exponentially.[121] It was concluded that red light lasted for several minutes without RE traps. The PSL of SrS:Yb^{2+} was also recorded simultaneously at different stimulation times. When the sample was irradiated with excitation at 465 nm for 10 min, the PL intensity was observed to decline with increasing stimulation time supporting the non-existence of up-conversion process. It was proposed that luminescence arose as a result of release of accumulated energy in the traps of SrS:Yb^{2+}. From Fig. 28, it was noticed that PSL emission spectrum of SrS:Yb^{2+} was concurrent with the LPL excited by 465 nm indicating the involvement of same energy level in the two cases. In order to explain the concept behind LPL and PLS phenomena in SrS:Yb^{2+}, a mechanism was proposed by Yang et al. according to which the energy levels of Yb^{2+} in SrS were located near the bottom of the conduction band. Based upon the fact that the phosphors contained a small amount of dopant (Yb^{3+}) ions, they postulated the presence of deep traps T_B, which were due to crystal defects formed by Yb^{3+} ions. The shallow traps T_A were derived from the intrinsic defects formed during the synthesis of SrS:Yb^{2+}. Thus, processes of LPL and PSL

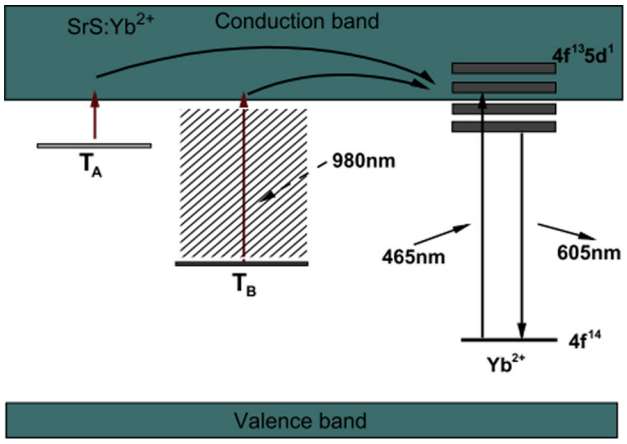

Fig. 29. LPL and PSL mechanisms in SrS:Yb^{2+} phosphor. Reprinted from "A novel Yb^{2+} doped SrS long persistent luminescence phosphors" by Yang et al.[110]

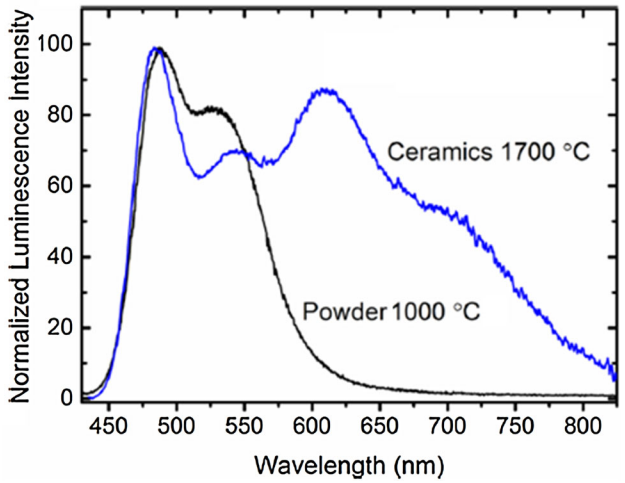

Fig. 30. Normalized luminescence spectra of SrS:Ce sample at an excitation wavelength of 425 nm. Reprinted from "Anomalous red and infrared luminescence of Ce^{3+} ions in SrS:Ce sintered ceramics" by Kulesza et al.[125]

were described in terms of promotion of ground state ($4f^{14}$) electrons of Yb^{2+} ions to excited state ($4f^{13}5d^{1}$) and conduction band under 465 nm excitation. Then the electrons were free to move in conduction band. When the free electrons came across the traps T_A and T_B, they were captured by traps. This process was understood as a mechanism of storing energy. When the 465 nm light source was withdrawn, the shallow traps T_A released the trapped electrons to conduction band gradually at RT, while the deep traps T_B needed additional energy (980 nm photons) to enable trapped electrons to escape from the traps T_B. Once the electrons were freed from the traps, they jumped from excited state ($4f^{13}$ $5d^{1}$) to ground state ($4f^{14}$) and emitted photons (Fig. 29).

SrS:Ce Sintered Ceramics: Red and IR Luminescence

SrS:Ce is a well known luminescent material emitting highly bright blue-green emission in the 450–650 nm wavelength range. The narrow band gap energy (4.20 eV) of SrS allows to excite it with standard light sources either directly or indirectly followed by a subsequent transfer of the acquired energy to the activator. In case of Ce^{3+} doped SrS, both the mechanisms can be adopted that open new avenues for research on SrS:Ce films for EL devices. SrS:Ce has limited applications due to its hygroscopic nature; however, there are reports[23] that recommend that this drawback is not a big issue, and in spite of it, these phosphors can be employed for many practical uses. Recently, CaS:Ce^{3+} and SrS:Eu^{2+} were reported to be potentially useful for many practical purposes.[122] Literature suggests that for higher content of Ce in the spectra of SrS and CaS, the peaks shifted towards higher wavelength side by 20–40 nm. It was attributed to the formation of Ce^{3+} pairs/clusters.[123] On the basis of their electron paramagnetic resonance (EPR) measurements, Hutti et al.[124] reported interactions between Ce^{3+} ions in the samples having more than 0.2% of Ce. Thus, excitation spectra of the red-shifted emissions were found quite similar to the spectrum of conventional Ce^{3+} luminescence. Kulesza et al.[125] prepared high-density SrS:Ce sintered ceramic material in reducing atmosphere of CO for the first time and reported their unique spectroscopic properties. As the authors claimed, their sintered ceramics exhibited a Ce^{3+} luminescence of an entirely different origin peaking around 620 nm. This research group compared the luminescence spectra of SrS:Ce in powder and pellet forms synthesized at 1000°C and 1700°C respectively. As shown in Fig. 30, the powder sample showed well-recognized luminescence with maxima falling around 480 nm and covering the 450–650 nm range of wavelengths. On the other hand, the spectrum of pellet sample was wider, which was accompanied by a well structured and equally intense emission band located in the range 550–800 nm and peaking at 620 nm.

In order to explain the luminescence spectra of newly identified SrS:Ce sintered pellets, authors recorded PLE and compared it with regular luminescence emitted at 480 nm. It was seen (Fig. 31) that the PLE spectrum of red-IR luminescence was completely different from the conventional one. When excited at 380 nm, the spectrum displayed an intense emission band peaking around 620 nm, which composed of two overlapping components splitted by 2040 cm^{-1}. This was resulted due to spin–orbit splitting of the Ce^{3+} ground levels into the $^2F_{5/2}$ and $^2F_{7/2}$. When excited with 520 nm, almost the same emission was generated into the lowest-energy excitation band of the red-IR luminescence. To know more about the luminescence features of SrS:Ce pellets, the authors performed

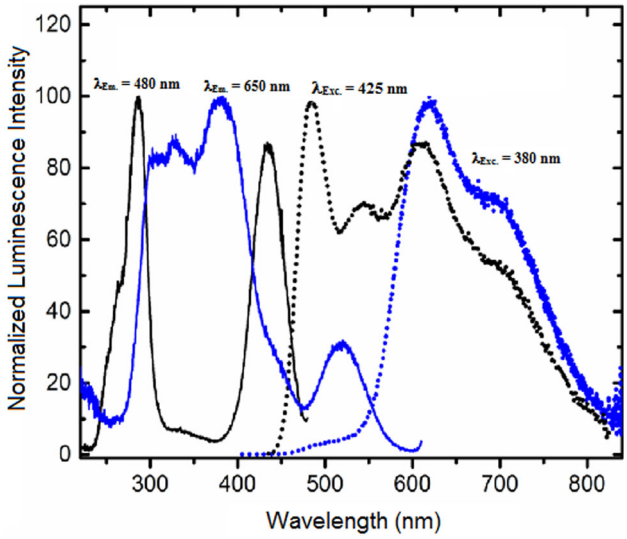

Fig. 31. RT normalized excitation spectra of 480 nm and 650 nm emissions (solid lines) and emission spectra excited at 380 nm and 425 nm wavelength (dotted lines) of SrS:Ce ceramics. Reprinted from "Anomalous red and infrared luminescence of Ce^{3+} ions in SrS:Ce sintered ceramics" by Kulesza et al.[125]

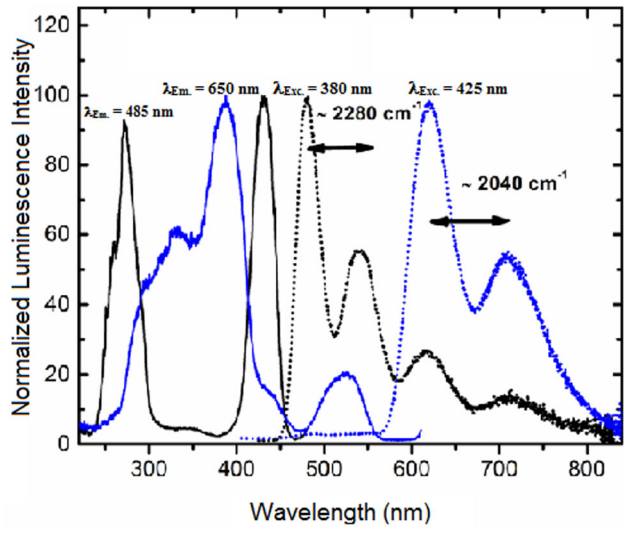

Fig. 32. Normalized low temperature (25 K) emission and excitation spectra revealing existence of two different Ce^{3+} luminescence centers in SrS:Ce ceramics. Reprinted from "Anomalous red and infrared luminescence of Ce^{3+} ions in SrS:Ce sintered ceramics" by Kulesza et al.[125]

the same experiments with SrS:Ce ceramic samples at different temperatures, the results of which are shown in Fig. 32. Both excitation and emission spectra appeared to be quite similar to those recorded at RT (Fig. 31), with the main deference being a much better splitting of the luminescent components. Excitation at 425 nm produced four well-resolved bands in the spectral region 450–800 nm; however, excitation at 380 nm resulted only in the red-IR luminescence comprising of two

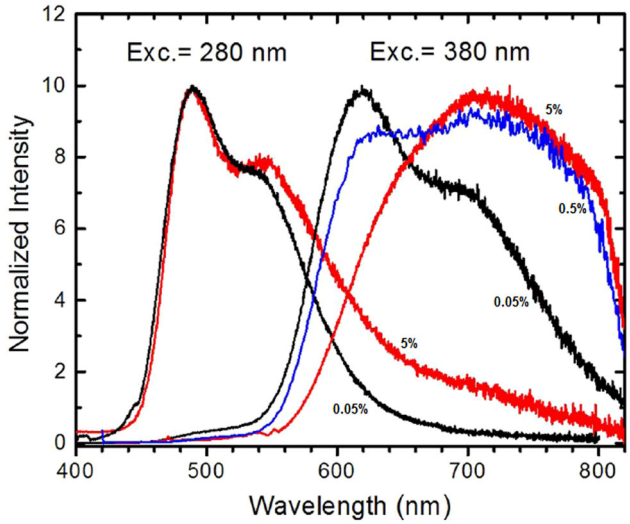

Fig. 33. Dependence of PL spectra of SrS:Ce sintered ceramics on the excitation wavelength and Ce concentration. Reprinted from "SrS:Ce and $LuPO_4$:Eu sintered ceramics: Old phosphors with new functionalities" by Zych et al.[126]

components, which coincided with the two long-wavelength constituents of the emission excited at 425 nm. This clarified that excitation at 425 nm gave rise to emissions from both centers, while upon 380 nm excitation, only the anomalous one excited producing its characteristic red-IR luminescence. In conclusion, it can be accomplished that apart from showing regular blue-green luminescence peaking at 480 nm, SrS:Ce ceramics presented an intense and never reported emission located in red and IR part of spectrum peaking at 620 nm. It is worth reporting that long-wavelength luminescence possessed all the characteristics of the Ce^{3+} ions with a decay time of 79 ns at 25 K. The irregular luminescence was proposed to be originated from agglomeration of point defects resulting due to high temperature sintering and enormous mass transfer.

SrS:Ce Sintered Ceramic: Old Phosphor with New Functionalities

Zych et al.[126] recently published a paper in which they projected SrS:Ce sintered ceramic with new possibilities. They suggested that red-IR band in the luminescence spectrum of SrS:Ce ceramics (sizes about 1–2 μm) may be useful as photo- and radioluminescence agents. In recent times, x-ray phosphors and scintillators have offered numerous applications in the field of imaging, especially in medical imaging. Storage phosphors belong to a special class of luminescent materials that absorb ionizing radiation without emission of light.[101] Figure 33 presents PL spectra of SrS:Ce ceramic excited at different wavelengths and varied concentration of activator (0.05%, 0.5%, and 5%). Upon excitation at 280 nm, the three samples showed emission bands quite similar to SrS:Ce powders. As

the activator (Ce) concentration was increased, a long-wavelength luminescent tail was witnessed. Its intensity was, however, low even for the highest doped (5%) specimen. On the other hand, excitation at 380 nm produced an entirely new emission that covered a broad range of wavelengths in the orange, red and to some extent in IR region of spectrum (550–830 nm). There was obtained considerable advancement of the long wavelength band position and shape as the activator concentration increased from 0.05% to 5%. The emission peak moved from 620 nm to 710 nm. For the intermediate concentration (0.5%) of activator, the spectrum was flat over the 520–720 nm range. The sample containing 0.5% of Ce showed transitional behavior between the lower and higher concentration systems. Thus, this study resulted in a new emitting center giving the red-infrared (R-IR) luminescence generated by means of sintering at 1700°C.

FUTURE ASPECTS

Recently, there have been investigations on various properties of RE doped SrS phosphor; however, the possibilities to explore them further are limitless. An impression has been dealt about the historical development of phosphors for displays and why sulfides have attained a renewed interest as luminescent materials for solid-state lighting. Making the above argument as the base, it is quite sure that persistent luminescent research has a promising prospect.

The inquisitiveness of the researchers for new and better materials with RE ions as activators continues. In recent times, it has turned to other host materials, based on the developments in LED conversion phosphors. Moreover, the pursuit to unravel the mechanism behind persistent luminescence has entered a new dimension. Different models have been proposed in the past few decades with only a small number of experimental backup, but only presently researchers have started applying innovative techniques that could authenticate or negate these theories. An improved comprehension of the accurate mechanism is decisive for the progress of practical applications such as emergency signs, traffic signage, dials and displays, textile printing, medical diagnostics, and more. RE ions activated LLPs will play a crucial function in the bright future of persistent luminescence. Indeed, the combination of highly luminescent Eu^{2+} ions and a sulfide host allow the broad excitation and emission bands that are ideal for wavelength conversion in LEDs for solid-state white lighting. PL intensity of the SrS:Ce^{3+} nanocrystalline phosphor at 254 nm excitation increases threefold, which makes it an excellent candidate for the practical application as a scintillator for gamma or x-rays, in high energy physics as a rack detector and also for applications in the medical field.

The discussed phosphor recommends an additional suitability to be excited with 355 nm (which falls under emission of a black light source) and can further be investigated for various applications. To make a statement regarding the correct nature of trapping centers or defects, we recognize the significance of other studies, viz. thermally stimulated conductivity (TSC), electron spin resonance (ESR), etc.

This paper on the optical properties of RE doped SrS phosphor presents a concise, but appealing overview of the state of the art in research on phosphors and offers many opportunities for future research. Despite the comparatively small size of the phosphor research community, there is a strong drive toward the design and characterization of specific phosphors, the development of new application areas, and a more profound understanding of the trapping and release mechanisms.

CONCLUSIONS

In this review, we have made an attempt to give an account of the recent history of RE doped SrS for a wide range of optical properties. This material has proven to be relatively better phosphor (bulk and thin films) as far as applications in various fields are concerned. SrS doped with different RE elements can be explored to optimize the performance of EL display devices. While developing two component phosphor system (SrS:Cu,Ag), in the coupling mechanism between Cu and Ag ions in SrS thin films, one ion gets excited and other de-excited. The decay time is found more in case of Cu doped SrS. The PSL intensity of SrS:Eu,Sm was found to be dose dependent, which was favourable for SrS:Eu,Sm to be used as a two dimensional imaging sensor. The absence of any peak in TL spectrum signifies the presence of deeper trapping levels. In Pr^{3+} doped SrS, the natural vacancies and defects play crucial role since in their presence, new electronic states can exist within the band-gap leading to greater number of electronic transitions. The synthesis of nanocrystalline $Ca_{1-x}Sr_xS$:Eu with a solvothermal method is advantageous to tune the emission spectrum by changing the composition and the potential to create entirely new types of luminescent devices. In nanocrystalline SrS:Ce, size quantization dominates and supports the improvement in its electrical, optical, chemical, and mechanical properties. The absorption studies reveal the indirect band gap nature of SrS:Ce thin films. Also, the band gap value is blue-shifted due to QSE. Eu^{2+} doped SrS can be a potential candidate for fabrication of white LEDs. It exhibits a broadband absorption in visible region, and hence can fulfill requirements for blue LED chips. In comparison to experimental band gap value (2.55 eV) of SrS:Yb, the generalized gradiant approximation gave a slightly lower value of the same. As a whole, it can be concluded that SrS doped with different RE elements shows exciting

properties that can be applied for developing newer applications.

ACKNOWLEDGEMENT

The authors are thankful to C.J. Summers, W. Park, L. Lu, J. E. Van Haecke, Shreyas S. Pitale, D. Poelman, Vinay Kumar, K. Suresh, A.Vij, Y. Yang, D. Kulesza, E. Zych, their co-workers and the publishers of the journals (Elsevier B.V. Netherland, The Electrochemical Society USA, Springer Publishing Company USA, Hindawi Publishing Corporation and American Chemical Society), whose works have been reviewed here. Also, authors are grateful to Dr. Anoop Tiwari, Department of Humanities and Social Sciences, NIT Raipur, India for rendering professional help in language corrections.

REFERENCES

1. W.M. Yen, S. Shionoya, and H. Yamamoto, *Phosphor Handbook*, 2nd ed. (Boca Raton, FL, USA: CRC Press, 2007).
2. W.M. Yen and M.J. Weber, *Inorganic Phosphors: Compositions, Preparation and Optical Properties* (Boca Raton, FL, USA: CRC Press, 2004).
3. H.W. Leverenz, *An Introduction to Luminescence of Solids* (New York, NY, USA: Wiley, 1950).
4. T. Sidot, *C. R. Acad. Sci.* 62, 999 (1866).
5. E. Wiedemann and U. Fluorescenz, Ueber Fluorescenz und Phosphorescenz I. Abhandlung. *Ann. Phys.* 34, 446 (1888).
6. M. Fox, *Optical Properties of Solids*, 2nd ed. (Oxford: Oxford University Press, 2004), p. 2.
7. T.H. Gfroerer, *Encyclopedia of Analytical Chemistry* (Hoboken: Wiley, 2006).
8. M.A. Chamarro, C. Gourdon, and P. Lavallard, *Semicond. Sci. Technol.* 8, 1868 (1993).
9. W.-M. Li (Thesis, University of Helsinki, Finland, 2000).
10. G. Blasse and B.C. Grabmaier, *Luminescent Materials* (Berlin: Springer, 1994), p. 136.
11. N.A. Vlasenko and Y.A. Popkov, *Opt. Spektrosk.* 8, 81 (1960).
12. V. Shanker, S. Tanaka, M. Shiiki, H. Deguchi, H. Kobayashi, and H. Sasakura, *Appl. Phys. Lett.* 45, 960 (1984).
13. W.A. Barrow, R.E. Coovert, and C.N. King, *SID Symposium Digest of Technical Papers* (1984), p. 249.
14. S.Tanaka, V. Shanker, M Shiiki, H. Deguchi, and H. Kobayashi, *SID Symposium Digest of Technical Papers* (1985), p. 255.
15. J.E. Van Haecke, P.F. Smet, and D. Poelman, *Spectrochim. Acta Part B Atom. Spectrosc.* 59, 1759 (2004).
16. J.E. Van Haecke, P.F. Smet, and D. Poelman, *J. Electrochem. Soc.* 152, 225 (2005).
17. D. Poelman, R. Vercaemst, R.L. Van Meirhaeghe, W.H. Laflere, and F. Cardon, *J. Lumin.* 75, 1751 (1997).
18. T. Yoshioka, Y. Sano, K. Nunomura, C. Tani, *SID Symposium Digest of Technical Papers* (1989), p. 313.
19. D. Poelman, R.L. Vanmeirhaeghe, W.H. Laflere, and F. Cardon, *J. Lumin.* 52, 259 (1992).
20. D. Poelman, R. Vercaemst, R.L. Vanmeirhaeghe, W.H. Laflere, and F. Cardon, *J. Lumin.* 65, 7 (1995).
21. D. Poelman, D. Wauters, R.L. Van Meirhaeghe, and F. Cardon, *Solid State Commun.* 113, 405 (2000).
22. D. Poelman, R. Vercaemst, R.L. Vanmeirhaeghe, W.H. Laflere, and F. Cardon, *Jpn. J. Appl. Phys., Part 1* 32, 3477 (1993).
23. P.F. Smet, I. Moreels, Z. Hens, and D. Poelman, *Materials* 3, 2834 (2010).
24. F. Nakano, N. Uekura, Y. Nakanishi, Y. Hatanaka, and G. Shimaoka, *Appl. Surf. Sci.* 121, 160 (1997).
25. P. Benalloul, C. Barthou, J. Benoit, L. Eichenauer, and A. Zeinert, *Appl. Phys. Lett.* 63, 1954 (1993).
26. P. Smet, D. Wauters, D. Poelman, and R.L. Van Meirhaeghe, *Solid State Commun.* 118, 59 (2001).
27. S.S. Sun, E. Dickey, J. Kane, and P.N. Yocom, *Proceedings of the 17th International Display Research Conference* (1997), p. 301.
28. A. Vij, R. Kumar, F. Singh, and N. Singh, *AIP Conf. Proc.* 1349, 491 (2011).
29. A. Vij, S. Gautama, V. Kumar, R. Brajpuriyad, R. Kumar, N. Singh, and K.H. Chae, *Appl. Surf. Sci.* 264, 237 (2013).
30. W.A. Barrow, R.E. Coovert, and C.N. King, *Digest 1984 SID International Symposium* (1984), p. 249.
31. S.S. Sun, E. Dickey, J. Kane, and P. Yocom, *Conference Record of the 1997 International Display Research Conference* (1997), p. 301.
32. K. Ohmi, T. Fujiwara, H. Fukada, S. Tanaka, and H. Kobayashi, *J. Cryst. Growth* 214, 950 (2000).
33. A. Kale (Thesis, University of Florida, 2003).
34. C.J. Summers, B.K. Wagner, W. Tong, W. Park, M. Chaichimansour, and Y.B. Xin, *J. Cryst. Growth* 214/215, 918 (2000).
35. J. Kane, W. Harty, M. Ling, and P.N. Yocom, *SID '85 Digest* (SID: Santa Ana, 1985), p. 163.
36. S.S. Sun, E. Dickey, J. Kane, and P.N. Yocom, *SID'97 Conference Record* (SID: Santa Ana, 1997), p. 301.
37. W. Park, T.C. Jones, W. Tong, B.K. Wagner, C.J. Summers, and S.S. Sun, *Proceedings of the Third International Conference on Science and Technology of Display Phosphors* (1997).
38. N. Miura, M. Kawanishi, H. Matsumoto, and R. Nakano, *Jpn. J. Appl. Phys.* 38, 11B (1999).
39. G. Runhong, N. Miura, H. Matsumoto, and R. Nakano, *J. Rare Earths* 24, 119 (2006).
40. W. Park, T.C. Jones, E. Mohamed, C.J. Summers, and S.S. Sun, *Proceedings of the Fifth International Display Workshop* (1998), p. 613.
41. D.R. Vij, *Luminescence of Solids* (New York: Plenum Press, 1998), p. 4.
42. T.C. Jones, W. Park, and C.J. Summers, *Appl. Phys. Lett.* 75, 2398 (1999).
43. W. Park, T.C. Jones, and C.J. Summers, *Appl. Phys. Lett.* 74, 1785 (1999).
44. W. Park, T.C. Jones, and C.J. Summers, *J. Lumin.* 87/89, 1267 (2000).
45. D.L. Dexter, *J. Chem. Phys.* 21, 836 (1953).
46. H. Nanto, Y. Douguchi, J. Nishishita, M. Kadota, N. Kashiwagi, T. Shinkawa, and S. Nasu, *Jpn. J. Appl. Phys.* 36, 421 (1997).
47. L.H. Robins and J.A. Ruchman, *Phys. Rev. B* 57, 12094 (1998).
48. L.P. Lu, X.Y. Zhang, Q.S. Liu, X. Mi, and Z. Xiao, *J. Rare Earths* 22, 155 (2004).
49. H. Nanto, Y. Hirai, M. Ikeda, M. Kadota, J. Nishishita, S. Nasu, and Y. Douguch, *Proceedings of The 8th International Conference on Solid-state Sensors and Actuators, and Eurosensors IX Stockholm* (1995), p. 175.
50. H. Zhiyi, W. Yongsheng, S. Li, H. Yanbing, and X. Xurong, *Sci. China Ser A* 44, 1189 (2001).
51. L. Lu, X. Zhang, Z. Bai, X. Wang, X. Mi, and Q. Liu, *Adv. Powder Technol.* 17, 181 (2006).
52. L.S. Park and M.S. Im, *Mol. Cryst. Liq. Cryst.* 425, 319 (2004).
53. C. Wang, K. Tang, Q. Yang, C. An, B. Hai, G. Shen, and Y. Qian, *Chem. Phys. Lett.* 351, 385 (2002).
54. B. Sun, G. Yi, D. Chen, Y. Zhou, and J. Cheng, *J. Mater. Chem.* 12, 1194 (2002).
55. J.E. Van Haecke, P.F. Smet, K. De Keyser, and D. Poelman, *J. Electrochem. Soc.* 154, J278 (2007).
56. J.E. Van Haecke, P.F. Smet, and D. Poelman, *Spectrochim. Acta, Part B* 59, 1759 (2004).
57. C. Chartier, C. Barthou, P. Benalloul, and J.M. Frigerio, *Electrochem. Solid State Lett.* 9, 53 (2006).
58. P. Dorenbos, *J. Phys.: Condens. Matter* 15, 4797 (2003).

59. Y. Hu, W. Zhuanga, H. Ye, S. Zhanga, Y. Fanga, and X. Huang, *J. Lumin.* 111, 139 (2005).
60. R. Pandey and S. Sivaraman, *J. Phys. Chem. Solids* 52, 211 (1991).
61. C. Guo, B. Chu, M. Wu, and Q. Su, *J. Lumin.* 105, 121 (2003).
62. Y.H. Lee, B.K. Ju, T.H. Yeom, D.H. Kim, and T.S. Hahn, *J. Appl. Phys.* 75, 1754 (1994).
63. S.S. Pitale, S.K. Sharma, R.N. Dubey, M.S. Qureshi, and M.M. Malik, *J. Lumin.* 128, 1587 (2008).
64. F.S. Kao and T.M. Chen, *J. Solid State Chem.* 156, 84 (2001).
65. D.R. Vij, *Thermoluminescent Materials* (NJ, USA: PTR Prentice Hall, 1993).
66. A. Khare, *J. Lumin.* 130, 1268 (2010).
67. D. Poelman, J.E. Van Haecke, and P.F. Smet, *J. Mater. Sci.: Mater. Electron.* 20, 134 (2009).
68. C.R. Wang, K.B. Tang, Q. Yang, C.H. An, B. Hai, G.Z. Shen, and Y.T. Qian, *Chem. Phys. Lett.* 351, 385 (2002).
69. M. Nazarov and C. Yoon, *J. Solid State Chem.* 179, 2529 (2006).
70. J.E. Van Haecke, P.F. Smet, and D. Poelman, *Spectrochim. Acta Part B At. Spectrosc.* 59, 1759 (2004).
71. E.I. Anila (Thesis, University of Calicut, Kerala, 2008).
72. V. Kumar, S.S. Pitale, M.M. Biggs, I.M. Nagpure, O.M. Ntwaeaborwa, and H.C. Swart, *Mater. Lett.* 64, 752 (2010).
73. P. Benalloul, C. Barthou, J. Benoit, A. Garcia, C. Fouassier, and E. Soininen, *Eur. Phys. J. Appl. Phys.* 9, 19 (2000).
74. V. Singh, M. Tiwari, T.K.G. Rao, and S.J. Dhoble, *Bull. Mater. Sci.* 28, 31 (2005).
75. W.M. Yen, S. Shionaya, and H. Yamamoto, *Practical Applications of Phosphors* (Boca Raton: CRC Press, 2006).
76. K. Suresh, K.V.R. Murthy, C.A. Rao, N.V.P. Rao, and I.S.R.N. Cond, *Mater. Phys.* 2011, 392917 (2011).
77. Y. Hu, W. Zhuang, H. Ye, S. Zhang, Y. Fang, and X. Huang, *J. Lumin.* 111, 139 (2005).
78. C. Karner, P. Maguire, J. McLaughlin, and S. Laverty, *Philos. Mag. Lett.* 76, 111 (1997).
79. J.Y. Choe, S.M. Blomquist, and D.C. Morton, *Appl. Phys. Lett.* 80, 4124 (2002).
80. P. Smet, D. Wauters, D. Poelman, and R.L.V. Meirhaeghe, *Solid State Commun.* 118, 59 (2001).
81. W.L. Warren, K. Vanheusden, D.R. Tallant, C.H. Seager, S.S. Sun, D.R. Evans, W.M. Dennis, E. Soininen, and J.A. Bullington, *J. Appl. Phys.* 82, 1812 (1997).
82. H. Heikkinen, L.S. Johansson, E. Nykänen, and L. Niinistö, *Appl. Surf. Sci.* 133, 205 (1998).
83. M.B. Sahana, C. Sudakar, G. Setzler, A. Dixit, J.S. Thakur, G. Lawes, R. Naik, V.M. Naik, and P.P. Vaishnava, *Appl. Phys. Lett.* 93, 231909 (2008).
84. S.K. Mishra, R.K. Srivastava, S. Prakash, R.S. Yadav, and A. Panday, *J. Alloys Compd.* 513, 118 (2012).
85. D. Beena, K. Lethy, R. Vinodkumar, A. Detty, V.M. Pillai, and V. Ganesan, *J. Alloys Compd.* 489, 215 (2010).
86. E.I. Anila, A. Aravind, and M.K. Jayaraj, *Nanotechnology* 19, 145604 (2008).
87. A. Vij, S. Gautama, R. Kumar, A.K. Chawla, R. Chandra, N. Singh, and K.H. Chaea, *Appl. Surf. Sci.* 264, 237 (2013).
88. A. Vij, S. Gautama, R. Kumar, A.K. Chawla, R. Chandra, N. Singh, and K.H. Chaea, *J. Alloys Compd.* 527, 1 (2012).
89. S. Sze, *Physics of Semiconductor Devices* (New York: Wiley, 2004), p. 39.
90. A. Vij, S. Singh, R. Kumar, S.P. Lochab, V.V.S. Kumar, and N. Singh, *J. Phys. D Appl. Phys.* 42, 105103 (2009).
91. R.N. Bhargava, D. Gallagher, X. Hong, and A. Nurmikko, *Phys. Rev. Lett.* 72, 416 (1994).
92. D. Li, B.L. Clark, and D.A. Keszler, *Chem. Mater.* 12, 268 (2000).
93. W.L. Warren, K. Vanheusden, D.R. Tallant, C.H. Seager, S.S. Sun, D.R. Evans, W.M. Dennis, E. Soininen, and J.A. Bullington, *J. Appl. Phys.* 82, 1812 (1997).
94. B. Huttl, U. Troppenz, K.O. Velthaus, C.R. Ronda, and R.H. Mauch, *J. Appl. Phys.* 78, 7282 (1995).
95. S. Mhin, J. Ryu, K. Kim, G. Park, H. Ryu, K. Shim, T. Sasaki, and N. Koshizaki, *Nano Res. Lett.* 4, 888 (2009).
96. S. Mishra, A. Khare, D.S. Kshatri, and S. Tiwari, *Mater. Sci. Semicond. Process.* 40, 230 (2015).
97. S. Mishra, A. Khare, D.S. Kshatri, and S. Tiwari, *Superlattices Microstruct.* 86, 73 (2015).
98. S. Mishra, D.S. Kshatri, A. Khare, S. Tiwari, and P.K. Dwivedi, *Mater. Lett.* 183, 191 (2016).
99. D.S. Kshatri and A. Khare, *J. Lumin.* 155, 257 (2014).
100. N. Yamashita, Y. Michitsuji, and S. Asano, *J. Electrochem. Soc.* 134, 2932 (1987).
101. P. Thiyagarajan, M. Kottaisamy, and M.S. Ramachandra Rao, *Mater. Res. Bull.* 42, 753 (2007).
102. E. Malchukova and B. Boizot, *J. Rare Earths* 32, 217 (2014).
103. A.A. Setlur, *Electrochem. Soc. Int.* 16, 32 (2009).
104. C. Bouvy, W. Marine, R. Sporken, and B.L. Su, *Chem. Phys. Lett.* 428, 312 (2006).
105. O.R. Ochoa, C. Colajacomo, E.J. Witkowski, J.H. Simmons, and B.G. Potter, *Solid State Commun.* 98, 717 (1996).
106. D. Yuan, G.S. Yi, and G.M. Chow, *J. Mater. Res.* 24, 2042 (2009).
107. R.E. Rojas-Hernandez, F. Rubio-Marcos, E. Enríquez, M.A. De La Rubia, and J.F. Fernandez, *RSC Adv.* 5, 42559 (2015).
108. A. Vij, R. Kumar, A.K. Chawla, S.P. Lochab, R. Chandra, and N. Singh, *Opt. Mater.* 33, 58 (2010).
109. J. Hou, W. Jiang, Y. Fang, and F. Huang, *J. Mater. Chem. C* 1, 5892 (2013).
110. Y. Yang, X. Li, X. Su, Z. Li, L. Liu, Y. Liu, J. Zhang, C. Mi, and F. Yu, *Opt. Mater.* 36, 1822 (2014).
111. B. Lei, S. Yue, Y. Zhang, and Y. Liu, *Chin. Phys. Lett.* 27, 37201 (2010).
112. H.N. Luitel, T. Watari, R. Chand, T. Torikai, and M. Yada, *Opt. Lett.* 34, 1375 (2012).
113. Y.H. Jin, Y.H. Hu, L. Chen, A.J. Wang, and G.F. Ju, *Opt. Mater.* 35, 1378 (2013).
114. X. Sun, J. Zhang, X. Zhang, Y. Luo, and X.J. Wang, *J. Phys. D Appl. Phys.* 41, 195414 (2008).
115. Y.H. Wang, Y. Gong, X.H. Xu, and Y.Q. Li, *J. Lumin.* 133, 25 (2013).
116. D. Kulesza, J. Trojan-Piegza, and E. Zych, *Radiat. Meas.* 45, 490 (2010).
117. X.H. Xu, L.T. Yan, X. Yu, H.L. Yu, T.M. Jiang, Q. Jiao, and J.B. Qiu, *Mater. Lett.* 99, 158 (2013).
118. S. Labidi, H. Meradji, M. Labidi, S. Ghemid, S. Drablia, and F. El Haj Hassan, *Phys. Proc.* 2, 1205 (2009).
119. G.B. Bachelet and N.E. Christensen, *Phys. Rev. B* 31, 879 (1995).
120. E. Engel and S.H. Vosko, *Phys. Rev. B* 47, 13164 (1991).
121. W.B. Chen, Y.H. Wang, X.H. Xu, W. Zeng, and Y. Gong, *Solid State Lett.* 1, R17 (2012).
122. Y. Zhao, F.T. Rabouw, T. Puffelen, C.A. Walree, D.R. Gamelin, C. de Mello Donega, and A. Meijerink, *J. Am. Chem. Soc.* 136, 16533 (2014).
123. B. Hutti, U. Troppenz, K.O. Velthaus, C.R. Ronda, and R.H. Mauch, *J. Appl. Phys.* 78, 7282 (1995).
124. B. Hutti, U. Troppenz, H. Venghaus, R.H. Mauch, J. Kreissl, A. Garcia, C. Fouassier, P. Benalloul, C. Barthou, J. Benoit, F. Gendrom, and C. Ronda, *Mater. Sci. Forum* 263, 182 (1995).
125. D. Kulesza, J. Cybinska, L. Seijo, Z. Barandiarán, and E. Zych, *J. Phys. Chem. C* 119, 27649 (2015).
126. E. Zych, D. Kulesza, J. Zeler, J. Cybinska, K. Fiaczyk, and A. Wiatrowskac, *ECS J. Solid State Sci. Technol.* 5, R3078 (2016).